Mechanism of Generation of Spontaneous Miniature Outward Currents (SMOCs) in Retinal Amacrine Cells

Pratip Mitra and Malcolm M. Slaughter

Department of Physiology and Biophysics, School of Medicine, State University of New York at Buffalo, Buffalo, NY 14214

ABSTRACT A subtype of retinal amacrine cells displayed a distinctive array of K^+ currents. Spontaneous miniature outward currents (SMOCs) were observed in the narrow voltage range of −60 to −40 mV. Depolarizations above approximately −40 mV were associated with the disappearance of SMOCs and the appearance of transient (I_{to}) and sustained (I_{so}) outward K^+ currents. I_{to} appeared at about −40 mV and its apparent magnitude was biphasic with voltage, whereas I_{so} appeared near −30 mV and increased linearly. SMOCs, I_{to}, and a component of I_{so} were Ca^{2+} dependent. SMOCs were spike shaped, occurred randomly, and had decay times appreciably longer than the time to peak. In the presence of cadmium or cobalt, SMOCs with pharmacologic properties identical to those seen in normal Ringer's could be generated at voltages of −20 mV and above. Their mean amplitude was Nernstian with respect to $[K^+]_{ext}$ and they were blocked by tetraethylammonium. SMOCs were inhibited by iberiotoxin, were insensitive to apamin, and eliminated by nominally Ca^{2+}-free solutions, indicative of BK-type Ca^{2+}-activated K^+ currents. Dihydropyridine Ca^{2+} channel antagonists and agonists decreased and increased SMOC frequencies, respectively. Ca^{2+} permeation through the kainic acid receptor had no effect. Blockade of organelle Ca^{2+} channels by ryanodine, or intracellular Ca^{2+} store depletion with caffeine, eradicated SMOCs. Internal Ca^{2+} chelation with 10 mM BAPTA eliminated SMOCs, whereas 10 mM EGTA had no effect. These results suggest a mechanism whereby Ca^{2+} influx through L-type Ca^{2+} channels and its subsequent amplification by Ca^{2+}-induced Ca^{2+} release via the ryanodine receptor leads to a localized elevation of internal Ca^{2+}. This amplified Ca^{2+} signal in turn activates BK channels in a discontinuous fashion, resulting in randomly occurring SMOCs.

KEY WORDS: potassium channels • calcium-induced calcium release • ryanodine receptors • L-type calcium channels • ganglion cells

INTRODUCTION

In the vertebrate retina, amacrine and ganglion cells reside two synapses away from the photoreceptors. These third order neurons are driven by glutamatergic inputs from bipolar cells, and are the first neurons in the visual pathway that generate action potentials (Dowling and Werblin, 1969; Werblin and Dowling, 1969; Kaneko, 1970). Perhaps, because of their distinctive nonlinear membrane properties, these neurons have a large assortment of K^+ channels. We explored the properties and relationships between several K^+ channels found in one subtype of third order neuron: an amacrine cell subtype.

K^+ channels can be broadly categorized based on gating into voltage- and ligand-activated subtypes (Hille, 1992). A notable group amongst the ligand-activated are those gated by intracellular Ca^{2+}, the Ca^{2+}-activated K^+ channels (K_{Ca}), and their presence in retinal third order neurons has been documented (Lipton and Tauck, 1987; Latorre et al., 1989; Vergara et al., 1998; Wang et al., 1998). Cytoplasmic calcium ($[Ca^{2+}]_i$) responsible for the gating can arise either via influx through plasmalemmal channels or efflux from the ER (Zorumski et al., 1989; Kostyuk and Verkhratsky, 1994; Wisgirda and Dryer, 1994; Davies et al., 1996; Berridge, 1998; Marrion and Tavalin, 1998; Hurley et al., 1999; Imaizumi et al., 1999). The release of organelle Ca^{2+} is mediated primarily via two subtypes of intracellular Ca^{2+} channels. While both these channels are calcium sensitive, one subtype releases calcium in response to elevations in the levels of inositol 1,4,5-trisphosphate (IP_3) and the other responds primarily to elevations of cytoplasmic Ca^{2+} by Ca^{2+}-induced Ca^{2+} release (CICR)* (Fabiato, 1983; Berridge, 1993, 1998). The latter is sensitive to the plant alkaloid ryanodine, and is thus called the ryanodine receptor (RyR; Pozzan et al., 1994; Sutko and Airey, 1996; Zucchi and Ronca-Testoni, 1997). CICR is extremely well documented in cardiac muscle and also found in neurons (Kuba, 1994; Cheng

Pratip Mitra's present address is Department of Neuroscience, University of Minnesota, 6-145 Jackson Hall, 321 Church St. SE, Minneapolis, MN 55455.

Address correspondence to Malcolm Slaughter, Department of Physiology and Biophysics, State University of New York at Buffalo, 124 Sherman Hall, Buffalo, NY 14214. Tel.: (716) 829-3240; Fax: (716) 829-2344; E-mail: mslaught@buffalo.edu

*Abbreviations used in this paper: CICR, Ca^{2+}-induced Ca^{2+} release; DHP; dihydropyridine; KA, kainic acid; RyR, ryanodine receptor; SMOC, spontaneous miniature outward current; STOC, spontaneous transient outward current; TTX, tetrodotoxin; VGCC, voltage-gated calcium channel.

et al., 1996; Verkhratsky and Shmigol, 1996; Cohen et al., 1997; Jacobs and Meyer, 1997; Usachev and Thayer, 1997). It is thought to amplify calcium signals, such as those originating from influx via voltage-gated calcium channels (VGCCs) (Friel and Tsien, 1992). This amplified $[Ca^{2+}]_i$ signal may rise to magnitudes of several μM in local regions, activating membrane proteins such as Ca^{2+}-activated K^+ or Cl^- channels (Imaizumi et al., 1998; Gordienko et al., 1999). These CICR-generated localized elevations of $[Ca^{2+}]_i$, called "Ca^{2+} sparks," have been detected in smooth as well as cardiac muscle and there is evidence that sparks can activate clusters of large conductance K_{Ca} channels (BK subtype) (Nelson et al., 1995; Imaizumi et al., 1998; ZhuGe et al., 1999). In muscle cells under voltage clamp, K^+ fluxes through BK channels generated in this manner appear as random outward currents termed spontaneous transient outward currents (STOCs) (Benham and Bolton, 1986; Bolton and Imaizumi, 1996). STOCs are thought to govern the resting membrane potential in smooth muscle (Nelson et al., 1995; Jaggar et al., 1998). A similar mechanism, if existent in excitable neurons such as retinal amacrine cells, can potentially modulate neuronal excitability.

This study characterizes a subtype of retinal amacrine cell with respect to its K^+ current signature. In addition to voltage-activated K^+ currents, these neurons display a set of K_{Ca} currents with different temporal properties. These currents activate sequentially as the membrane potential of the neuron depolarizes. The K_{Ca} currents consist of a randomly occurring transient outward current, an early onset transient outward current, and a sustained outward current. The random outward current has properties similar to the STOCs seen in muscle cells, and in neurons are called spontaneous miniature outward currents (SMOCs) (Hartzell et al., 1977; Mathers and Barker, 1981, 1984; Satin and Adams, 1987; Fletcher and Chiappinelli, 1992; Merriam et al., 1999; Arima et al., 2001). This study reports the presence of SMOCs in retinal neurons and elucidates their mechanism of generation. A preliminary description of this work was presented by Mitra and Slaughter (2000).

MATERIALS AND METHODS

Retinal Cell Preparation

Aquatic tiger salamanders (*Ambystoma tigrinum*) obtained from Kons Scientific and Charles Sullivan were kept in tanks maintained at 4°C on a 12 h light/dark cycle. Experiments were performed on acutely isolated neurons by enzymatic dissociation of the retina (Lam, 1972; Bader et al., 1979; Pan and Slaughter, 1995). All procedures were performed in accordance with the United States Animal Welfare Act and the National Institutes of Health Guide for the Care and Use of Laboratory Animals (publication 85-23), and were approved by the University Animal Care Committee. Briefly, the animals were decapitated, pithed, and the eyes were enucleated. The cornea, lens, and vitreous were removed and the retina was isolated by separating it from the pigment epithelium. During this process the entire tissue was continuously immersed in normal amphibian Ringer's solution. The isolated retina was transferred to 350 μl of enzyme solution containing papain (12 U/ml; Worthington Biochemicals), deoxyribonuclease (0.28 mg/ml; Worthington Biochemicals), 5 mM L-cysteine, 1 mM EDTA dissolved in normal amphibian Ringer's, and adjusted to pH 7.4. The tissue was digested in enzyme solution for 40 min at room temperature and continuously oxygenated. The retina was rinsed five times with normal amphibian Ringer's solution, then gently shaken until the entire tissue dissociated. The cells were then plated onto lectin (0.4 mg/ml)-coated coverslips, allowed to settle for ~2 min, and then overlaid with normal amphibian Ringer and stored in a 13°C incubator. Experiments were performed within 4 h of dissociation. The cell type used for this study did not show any distinct morphological characteristics. However, they were identified by a distinct current signature exhibited when subjected to voltage clamp step depolarizations in normal Ringer (see RESULTS).

Experimental Setup and Data Acquisition

The plated coverslips were placed in a plexiglass recording chamber having a volume of 350 μl. One end of the chamber housed a suction tube connected to a peristaltic pump. The cells were viewed with an inverted microscope equipped with a 40× lens. Retinal cells were constantly superfused at room temperature with normal amphibian Ringer's solution bubbled with oxygen using a gravity fed perfusion system. The tubes of the gravity-fed perfusion system were connected to a common manifold, which held a wide bore patch pipette. This patch pipette was placed close to the cell during recordings, and solution exchanges could be achieved within 2–3 s. Control and test solutions were applied using this system. The drug effects described in this paper refer to steady-state effects usually obtained after 10–30 s of drug application. Data were acquired with an Axopatch-1C patch clamp amplifier (Axon Instruments, Inc.). Analogue signals were filtered at 5 KHz and sampled at 20 KHz with the DigiData 1200 analogue-to-digital board (Axon Instruments, Inc.) using Clampex 8 software (Pclamp 8; Axon Instruments, Inc.). Data were acquired using the whole cell variant of the patch clamp technique, in both the continuous voltage and current clamp modes (Hamill et al., 1981). Patch pipettes were fashioned from borosilicate glass and had resistances of ~5 MΩ when measured in bath solution. Data shown in this paper were corrected for pipette junction potential (~10 mV). Except for the voltage values given in Fig. 2, C and D, and associated text, where the voltage error due to series resistance (~10 MΩ) could have an impact on the interpretation, the voltages are uncorrected for series resistance. Since these neurons had high input resistances, leak subtraction was not necessary. This, along with the observation that at relatively negative voltages (−90 to −30 mV) the clamp currents were very small, suggested that the voltage error due to uncompensated series resistance was insignificant within this range. At more depolarized voltages the error can be significant. However, most of the arguments presented in this and the following paper do not rely on the absolute value of the voltage at these potentials. Cells were held at −80 mV except when specifically mentioned in the text.

SMOC Analysis

Repeated voltage steps of up to 500 ms duration elicited SMOCs, which were analyzed using Mini Analysis program (version 4.1.1; Synaptosoft, Inc.) and Origin (version 6.0; Microcal Software, Inc.). SMOCs were detected using either the automatic detection mode in the Mini Analysis software or manually by eye. SMOCs

seen in normal Ringer's appeared on a zero current baseline, whereas those seen at more depolarized levels with cobalt were superimposed on the voltage-activated current. Prior to SMOC detection, the value of the peak-positive deflection of the baseline current noise in the data group was set as a threshold to eliminate SMOCs that are indistinguishable from the baseline noise. Invariably 150–500 SMOCs were analyzed for each parameter. A minimum of 10 s of data from each cell displaying SMOCs were used for analysis of frequencies. Under conditions in which SMOC frequency was greatly reduced, the time was considerably longer. Invariably, each pharmacological manipulation was performed at different test voltages. Irrespective of the test voltage used, results were found to be qualitatively consistent in all cells tested. Average values given are from a subset of this entire dataset, comprising the cells that were examined at the reported voltage. Data are expressed as mean ± SEM. Statistical differences were ascertained by Students t test, where $P < 0.05$ was deemed significant.

Solutions

Normal amphibian Ringer's contained (in mM): 111 NaCl, 2.5 KCl, 1.8 $CaCl_2$, 1 $MgCl_2$, 10 dextrose, and 5 HEPES, buffered to pH 7.8 with NaOH and oxygenated. Co^{2+} Ringer was similar to normal Ringer's except that it contained 4–20 mM $CoCl_2$ and variable amounts of $CaCl_2$ (0–4.5 mM). Addition or removal of $CoCl_2$ or $CaCl_2$ to normal Ringer was accompanied by adjustment of the NaCl concentration to maintain osmolarity. Solutions mentioned as containing "0 mM Ca^{2+}" contain nominal unbuffered levels of calcium. Since only the bath calcium concentration was manipulated in this study, the notation "Ca^{2+}" used throughout the text, unless indicated otherwise, refers to external calcium. High K^+ Ringer's with or without the addition of Co^{2+} was prepared by equimolar substitution of NaCl with KCl. Recording pipettes contained (in mM): 110 K-gluconate, 5 NaCl, 1 $MgCl_2$, 5 EGTA, 5 HEPES adjusted to pH 7.4 with KOH. The pipette solution also contained an "ATP-regenerating cocktail" consisting of 4 mM ATP, 20 mM phosphocreatine, and 50 U/ml creatine phosphokinase. As noted in the RESULTS, bis (o-aminophenoxy)-N, N, N′, N′-tetraacetic acid (BA PTA, 10 mM) sometimes replaced EGTA in the internal solution. Ryanodine was dialyzed into the neurons by including it in the internal solution. Iberiotoxin, apamin, nifedipine, and S (−) BayK 8644 were obtained from Research Biochemicals, Inc. All other chemicals used in this study were obtained from Sigma-Aldrich. Dihydropyridines (DHPs) were prepared as 10 mM stock in ethanol and stored at −20°C. When using DHPs, care was taken to prevent exposure to light. Appropriate controls indicated that the final concentrations of ethanol used in this study did not have measurable effects. When using peptide toxins (iberiotoxin or apamin), BSA (0.1% wt/vol) was added to both control and toxin-containing solutions.

RESULTS

Electrophysiological Characterization of Cell Type

The neurons used for this study were classified as amacrine cells. They generated tetrodotoxin (TTX)-sensitive Na^+ action potentials, characteristic of both amacrine and ganglion cells (Werblin and Dowling, 1969). They did not fire spikes in a sustained manner in response to constant current injections, rather the spiking invariably accommodated after the first two or three action potentials, similar to that reported in earlier studies of amacrine cells (Barnes and Werblin, 1986; Eliasof et al., 1987). Moreover, cells in salamander retinal slice that show a similar current signature (see below) lie within the amacrine cell layer (unpublished data). On this basis, the neurons used in this study are tentatively identified as amacrine cells.

Fig. 1 A shows current recordings obtained from such a cell in normal Ringer's, under the whole cell voltage clamp. The cell was held at −80 mV and depolarized from −90 to 70 mV in 10 mV increments, in pulses of 500 ms. The family of traces obtained illustrates the current signature for this cell type. An inward TTX-sensitive (500 nM) Na^+ current (marked as I_{Na} in Fig. 1 A) activates at −30 mV. Large outward currents are activated in response to depolarization. These outward currents are primarily K^+ fluxes, as they reverse near 0 mV when bath Ringer's contained high K^+ equivalent to that in the recording pipette ($n = 11$; unpublished data). Since these cells have high input resistances, very small currents are seen in the voltage range between −90 and −70 mV. The first induced outward current appears at −60 mV. These currents, termed SMOCs, are spike-shaped and TTX-insensitive and occur within the narrow voltage range of −60 to −40 mV ($n = 12$). Fig. 1 B shows SMOCs elicited in normal Ringer's at −50 mV. SMOCs at −50 mV have a mean amplitude of 33 ± 0.5 pA, mean time to peak of 2.8 ± 0.1 ms, and a mean 95% decay time of 5.5 ± 0.1 ms (average of four cells, ~1,000 events). In this set of 1,000 analyzed events, SMOCs appeared at a frequency of 9.8 ± 0.5 Hz and the highest SMOC amplitude was 92 pA.

At −40 mV a transient outward current (I_{to}) appeared along with SMOCs (arrow at −40 mV in Fig. 1 A). Depolarization beyond −40 mV leads to the disappearance of SMOCs. Instead, the outward current trace shows a transient I_{to} along with a sustained outward current (I_{so}). The I_{so} starts to activate at −30 mV. Subsequent depolarizations indicate that the apparent proportion of I_{to} and I_{so} changes. This is shown in Fig. 1 C, wherein outward currents elicited at −20 and 40 mV are shown. The apparent magnitude of the transient I_{to} declines in amplitude (measured as the difference between the peak of I_{to} and the point at which it meets the I_{so}), whereas the sustained component (I_{so}) increases in amplitude as the cell is depolarized. Thus, there is a clear gradation in the appearance of outward current types with voltage. This is shown as a normalized current vs. voltage (I-V) plot in Fig. 1 D (averaged data from eight cells). Depolarization elicits SMOCs within the narrow voltage range of −60 to −40 mV, the I_{to} above −40 mV and the I_{so} above −30 mV, successively. The apparent magnitude of I_{to} initially increases, peaks at −20 mV, and then declines with further depolarization, whereas the I_{so} increases linearly with depo-

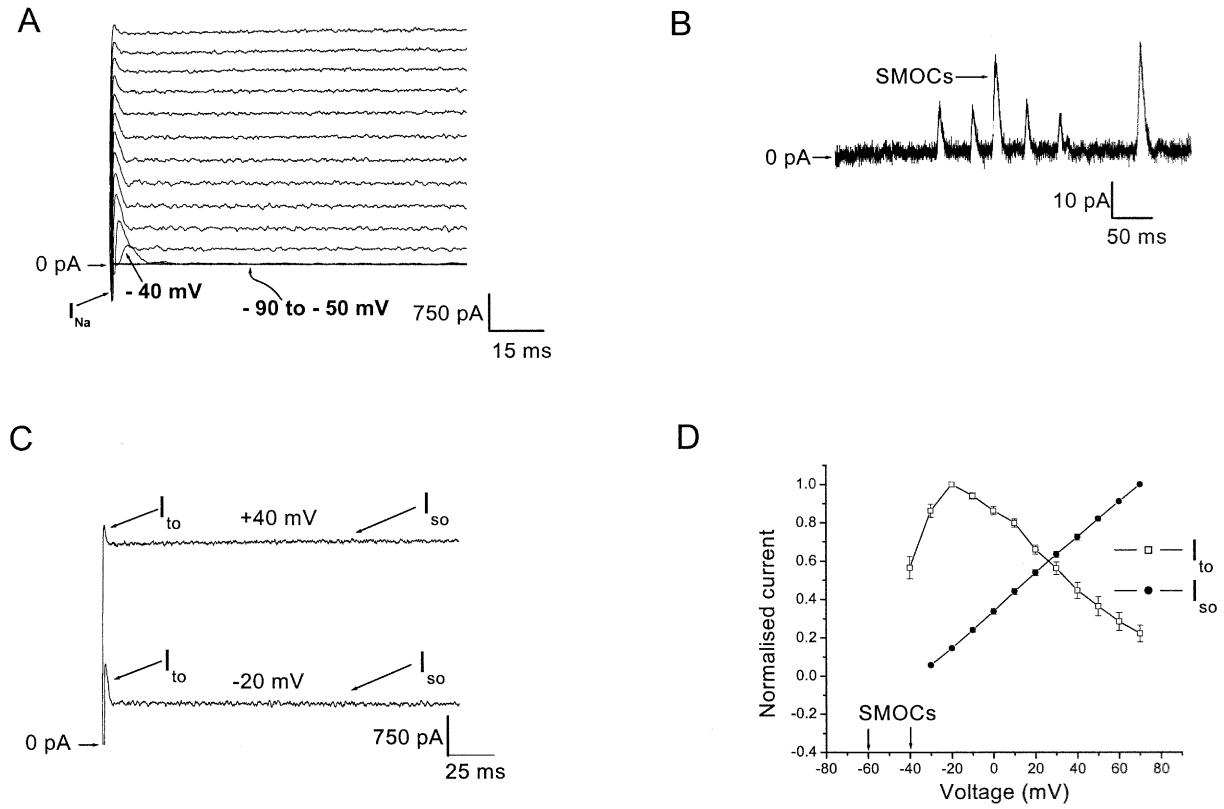

FIGURE 1. A subtype of retinal third order neurons shows a voltage-graded spectrum of outward currents. (A) Cell was held at −80 mV and currents were elicited in normal Ringer's by 500 ms depolarizing voltage steps from −90 to 70 mV in 10 mV increments. The sodium current is shown by arrow marked as I_{Na}. Note the appearance of the I_{to} at −40 mV (arrow). The magnification of the figure does not allow outward currents to be discerned between −90 to −50 mV (overlapping traces at these voltages shown by curved arrow). (B) At higher gain, SMOCs seen in normal Ringer's at −50 mV. (C) Whole cell outward currents elicited at −20 and 40 mV, comparing the amplitude of the sustained I_{so} and the apparent amplitude of the transient I_{to}. (D) Normalized I-V plot of the whole cell outward currents. Region enclosed within arrows indicates the voltage range of SMOC appearance. The magnitude of I_{so} (closed circles; measured at the end of the 500-ms pulse) and the apparent magnitude of I_{to} (open squares) have been normalized to their peak values. Data is an average of eight cells.

larization. All the subsequent data are recorded from cells with this prototypical current signature.

Calcium-dependent Outward Currents

The voltage-induced outward currents have an extracellular Ca^{2+}-dependent component. Fig. 2 A shows representative current recordings at 0 mV in normal Ringer's and in Ringer's containing 6 mM Co^{2+}/0 mM Ca^{2+}. Elimination of Ca^{2+} influx abolished I_{to} and reduced I_{so} at all voltages capable of eliciting these currents. The effects were fully reversible on switching back to control Ringer's. The subtracted trace at 0 mV is shown in Fig. 2 B, which is the Ca^{2+} influx–sensitive component, and is presumably mediated via K_{Ca} channels. It includes the entire I_{to} and a component of I_{so}, referred to as $I_{so\text{-}Ca}$ ($n = 8$). The residual current in 6 mM Co^{2+}/0 mM Ca^{2+} is defined as the Ca^{2+}-insensitive, voltage-dependent outward K^+ current, $I_{so\text{-}v}$ (Fig. 2 A, lower trace). Fig. 2 C shows a normalized I-V plot for the I_{so} (open circles) and its components, viz: $I_{so\text{-}v}$ (closed diamonds) and $I_{so\text{-}Ca}$ (open triangles) (average data from eight cells). As shown in Fig. 2 B, the $I_{so\text{-}Ca}$ is obtained by subtraction from the mean values of the I_{so} and $I_{so\text{-}v}$. The voltage values in Fig. 2, C and D, have been corrected for the drop across the series resistance (∼10 MΩ). The figure shows that beyond 0 mV, both I_{so} and $I_{so\text{-}v}$ increase in a relatively linear fashion, whereas $I_{so\text{-}Ca}$ shows a reduction in its slope. Fig. 2 D is a plot of the constituent $I_{so\text{-}Ca}$ (open triangles) and $I_{so\text{-}v}$ (closed diamonds) at each test voltage. Both components are expressed as a percentage of the total I_{so} at that particular voltage. Note the decline in the percentage of the $I_{so\text{-}Ca}$ component with increasing depolarization. The initial decline is due to the appearance of the $I_{so\text{-}v}$. However, its percentage continues to decrease at voltages beyond 0 mV; a range in which the $I_{so\text{-}v}$ I-V plot is relatively linear (see Fig. 2 C), suggesting that the channels comprising the $I_{so\text{-}v}$ are near maximal activation. This decline of the $I_{so\text{-}Ca}$ fraction would be expected if it was dependent on Ca^{2+} influx for its activation, since depolarization would tend to reduce the driving force for Ca^{2+} influx into the cell. At 0 mV, $I_{so\text{-}Ca}$ makes up 76.8 ± 2.9% of I_{so}. However, at 30 mV the $I_{so\text{-}Ca}$

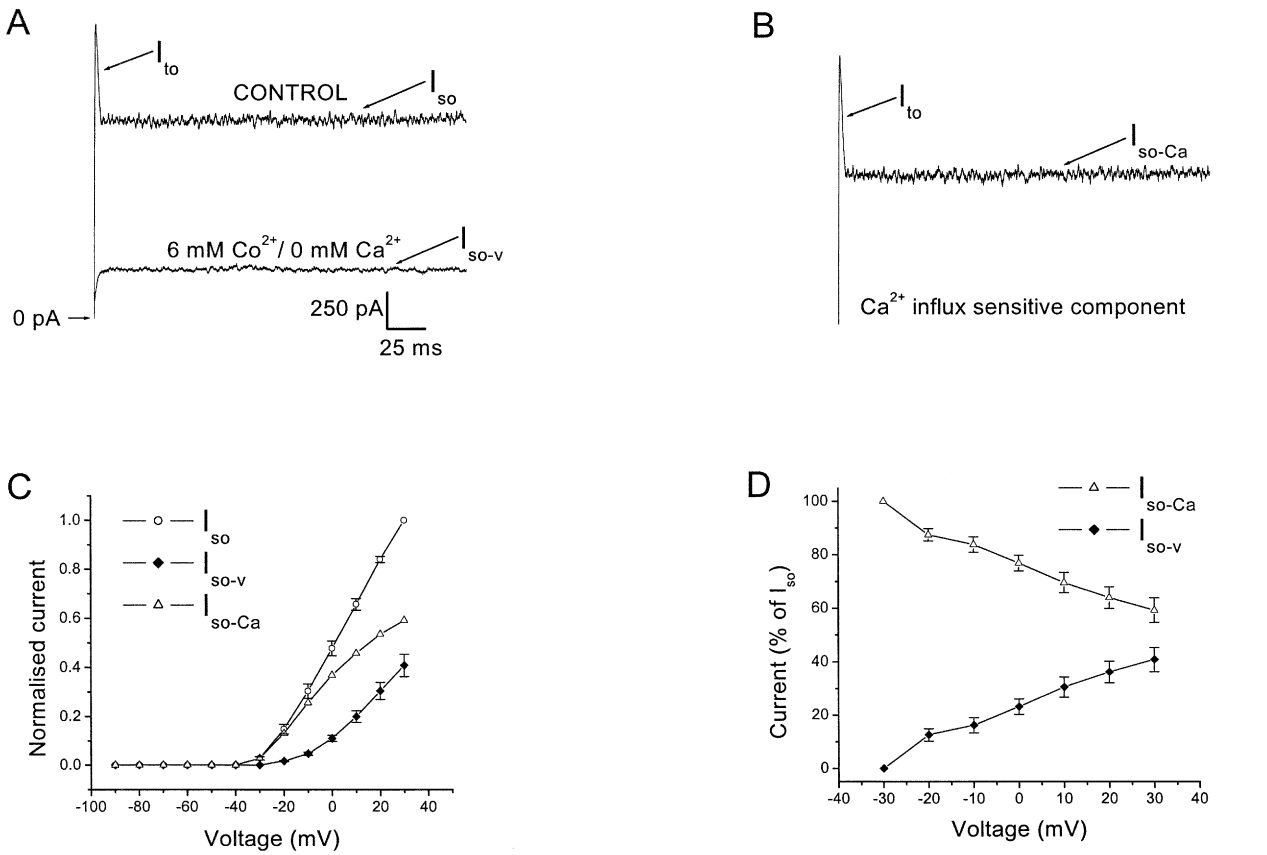

FIGURE 2. The voltage-induced outward currents have a Ca^{2+}-dependent component. Cells were held at −80 mV and currents elicited by 500 ms depolarizing voltage steps. (A) Current traces from a cell stepped to 0 mV in normal Ringer's or in 6 mM Co^{2+}/0 mM Ca^{2+} Ringer's. The residual current shown in the lower trace is the voltage-dependent component, I_{so-v}. (B) The subtracted trace (upper trace minus lower trace of Fig. 2 A) is the Ca^{2+}-dependent component. It includes the entire I_{to} and a component of the I_{so}, termed I_{so-Ca}. The scale for Fig. 2, A and B, are identical. (C) Normalized I-V plot for the I_{so} (open circles), I_{so-v} (closed diamonds), and I_{so-Ca} (open triangles). Currents have been normalized to the peak I_{so} value. The I_{so-Ca} is obtained by subtraction. Data is average of eight cells. (D) The I_{so-Ca} and I_{so-v} are plotted as a percentage of the total I_{so} at each voltage. Note the decline of the percentage of I_{so-Ca} with increasing depolarization. Data is an average of eight cells. The voltage values for the analyses in Fig. 2, C and D, have been corrected for the error due to the drop across the series resistance (∼10 MΩ).

makes up only 59.2 ± 4.6% of I_{so}; a shift in favor of the voltage-dependent component. SMOCs, similar to the I_{to} and I_{so-Ca}, were eliminated at −50 mV in the presence of 6 mM Co^{2+}/0 mM Ca^{2+} Ringer's, thus suggesting that they too were Ca^{2+} dependent (see next section).

Ca^{2+} Influx through VGCCs Is Required for the Generation of SMOCs

Reducing Ca^{2+} influx through VGCCs by the addition of inorganic blockers to normal Ringer's (6 mM Co^{2+}/ 1.8 mM Ca^{2+} Ringer's), led to the generation of SMOCs at −20 mV and above, while eliminating them at hyperpolarized voltages. Representative results are shown in shown in Fig. 3, A1 and A2 (V_{cmd} steps to −50 and 30 mV; $n = 20$). This is in contrast to the appearance of SMOCs in the narrow voltage range of −60 to −40 mV in normal Ringer's. SMOCs generated in 6 mM Co^{2+}/1.8 mM Ca^{2+} Ringer's at −10 mV had a mean amplitude of 158.2 ± 2.6 pA, mean time to peak of 3.7 ± 0.1 ms and a mean 95% decay time of 6.2 ± 0.1 ms (average data from ∼800 events in five cells). In this set of five cells used for analysis, SMOCs appeared at a frequency of 10.7 ± 0.40 Hz. A plot from a representative cell showing SMOC frequency versus inorganic blocker dose at 30 mV is shown in Fig. 3 B. Increasing the cobalt concentration, while maintaining 1.8 mM Ca^{2+}, reduced SMOC frequency. 20 mM cobalt eliminated SMOCs. In this cell, SMOC frequency was 21 ± 0.6 Hz at 4 mM Co^{2+} and was reduced to 7.2 ± 0.6 Hz at 8 mM cobalt ($P < 0.01$). Average data from five cells under similar conditions gave SMOC frequencies of 23.4 ± 1.2 Hz at 4 mM Co^{2+} and 7.9 ± 0.5 Hz under 8 mM Co^{2+} ($P < 0.01$). Addition of 100 μM Cd^{2+}, instead of Co^{2+}, also led to generation of SMOCs at depolarized voltages ($n = 15$). These effects of inorganic blockers were fully reversible on washout.

Fig. 3 C shows representative SMOCs generated at +30 mV in 6 mM Co^{2+}/1.8 mM Ca^{2+} Ringer's (Fig. 3 C1) and 6 mM Co^{2+}/0 mM Ca^{2+} Ringer's (Fig. 3 C2) solutions, respectively. The cell was exposed to the

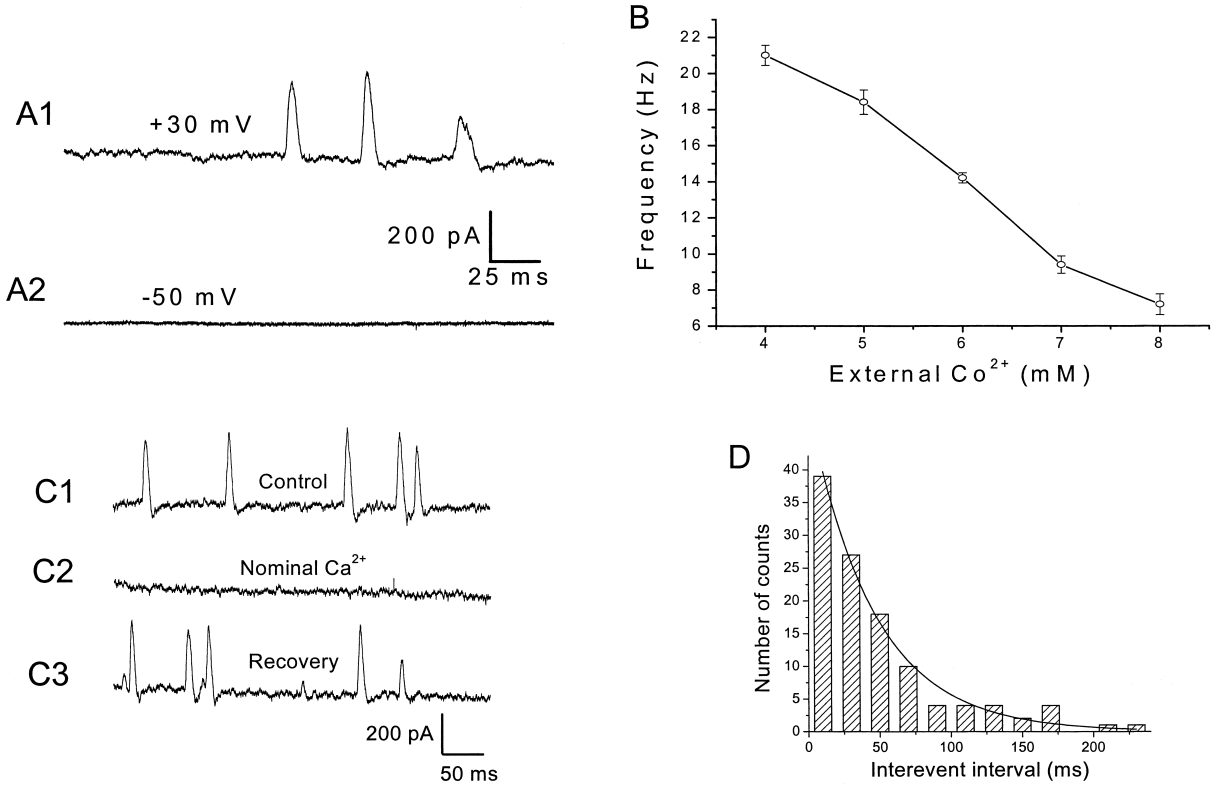

FIGURE 3. Ca^{2+} influx through VGCCs is required for the generation of SMOCs. (A) Representative traces showing addition of inorganic VGCC blocker (6 mM Co^{2+}) to Ringer's containing 1.8 mM Ca^{2+}-elicited SMOCs at 30 mV while eliminating them at −50 mV. SMOCs in A1 were superimposed on a baseline current of ~675 pA, whereas the trace in A2 is at the zero current level. (B) Effect of external cobalt concentration on SMOC frequency. Data are from a cell stepped to 30 mV in Ringer's containing 1.8 mM Ca^{2+} and varying levels of Co^{2+}. (C) Representative traces showing SMOCs generated at 30 mV in 6 mM Co^{2+}/1.8 mM Ca^{2+} Ringer's (C1), to 6 mM Co^{2+}/0 mM Ca^{2+} Ringer's (C2), then back to control solution containing 1.8 mM Ca^{2+} (C3). SMOCs in this representative cell were superimposed on a baseline current of ~1300 pA. (D) Interevent interval histogram for SMOCs generated at −10 mV in 6 mM Co^{2+}/1.8 mM Ca^{2+} Ringer's. The smooth line is a single exponential fit to the data.

nominally Ca^{2+}-free solution for 10 s and SMOCs were eliminated. However, these SMOCs were immediately reinstated on return to control 6 mM Co^{2+}/1.8 mM Ca^{2+} Ringer's (Fig. 3 C3) ($n = 15$). Subsequent sections show that release of intracellularly stored Ca^{2+} is involved in the SMOC generation pathway. Although prolonged (tens of minutes) exposure to Ca^{2+}-free solution can deplete the stores of Ca^{2+}, it is unlikely that 10 s exposures would cause such an effect. Moreover, brief exposures to low doses of caffeine (1–3 mM) after SMOCs were eliminated in nominally Ca^{2+}-free solution could reinstate SMOC-like activity ($n = 5$), suggesting the stores were replete under these conditions.

The dose-dependent reduction in SMOC frequency with increasing doses of inorganic blocker, and their elimination in nominal Ca^{2+}-containing solutions suggest that Ca^{2+} influx through VGCCs is involved in the SMOC generation pathway. Another possible route of Ca^{2+} influx into the cell is via receptor-operated channels (Betz, 1990; Gilbertson et al., 1991; Brorson et al., 1992; Kostyuk and Verkhratsky, 1994). In retinal third order neurons, the kainic acid (KA) receptor, a glutamate receptor subtype, has been shown to be permeable to Ca^{2+} (unpublished data; Otori et al., 1998; Taschenberger and Grantyn, 1998; Yoon et al., 1999). Addition of 50 μM KA to cells did not alter SMOC frequency ($n = 11$). SMOC frequency in 6 mM Co^{2+}/1.8 mM Ca^{2+} Ringer's at 30 mV was 5.3 ± 0.6 Hz. Addition of 50 μM KA resulted in a SMOC frequency of 5.2 ± 0.7 Hz (average data from three cells, difference between frequency values is not significant at $P < 0.05$). Increasing the driving force for KA-induced Ca^{2+} influx by generating SMOCs at −10 mV ($n = 3$) or −50 mV ($n = 5$) did not result in any significant change in frequency. These observations indicate that Ca^{2+} influx through VGCCs is necessary for SMOC generation.

SMOCs generated in the presence of cobalt were more stable, gave a better signal to noise ratio, and afforded a broader dynamic range of voltage activation. Due to these experimental advantages, it was far easier to unambiguously identify and quantitate SMOCs generated in this manner, as compared with those seen within a narrow voltage range in normal Ringer's. Therefore, the properties of SMOCs were examined in the presence of

cobalt. However, equivalent studies, when feasible, were done on SMOCs generated in normal Ringer's. The results of the two paradigms were qualitatively similar.

SMOCs occurred randomly irrespective of whether they were generated in normal or Co^{2+}-containing Ringer's. Fig. 3 D shows an interevent interval histogram for SMOCs generated in 6 mM Co^{2+}/1.8 mM Ca^{2+} Ringer's. The exponential interevent interval distribution obtained suggests the random nature of their occurrence.

Ca^{2+} Influx through High Voltage–activated (HVA) Ca^{2+} Channels Is Responsible for SMOC Generation

Since VGCCs are important for SMOC generation, the type of calcium channel was examined. SMOCs recorded in normal Ringer's are generated within a relatively hyperpolarized voltage range of −60 to −40 mV. It is possible that Ca^{2+} influx through low voltage–activated Ca^{2+} channels (T-type) might be involved. Lacking a pharmacological method of blocking this channel, a common biophysical approach is to inactivate T-type channels by holding the cells at depolarized voltages (Narahashi et al., 1987; Bean, 1989). With the holding potential at −80 mV, SMOCs generated at −50 mV in normal Ringer's had a frequency of 15.3 ± 1.6 Hz. Maintaining the holding potential at −50 mV resulted in a SMOC frequency of 13 ± 1.4 Hz (average from four cells; difference in frequencies was not significant at $P < 0.05$). Similarly, SMOCs generated in 6 mM Co^{2+}/1.8 mM Ca^{2+} by a step to −10 mV also failed to be eliminated when the holding voltage was −40 mV ($n = 3$; unpublished data). These results suggest that T-type channels are not involved in SMOC generation.

Fig. 4 A shows representative SMOC recordings obtained after a depolarization to −10 mV in 6 mM Co^{2+}/1.8 mM Ca^{2+} Ringer's in the absence (A1) and presence (A2) of 10 μM nifedipine, a blocker of L-type Ca^{2+} channels. Fig. 4 B shows that nifedipine produces

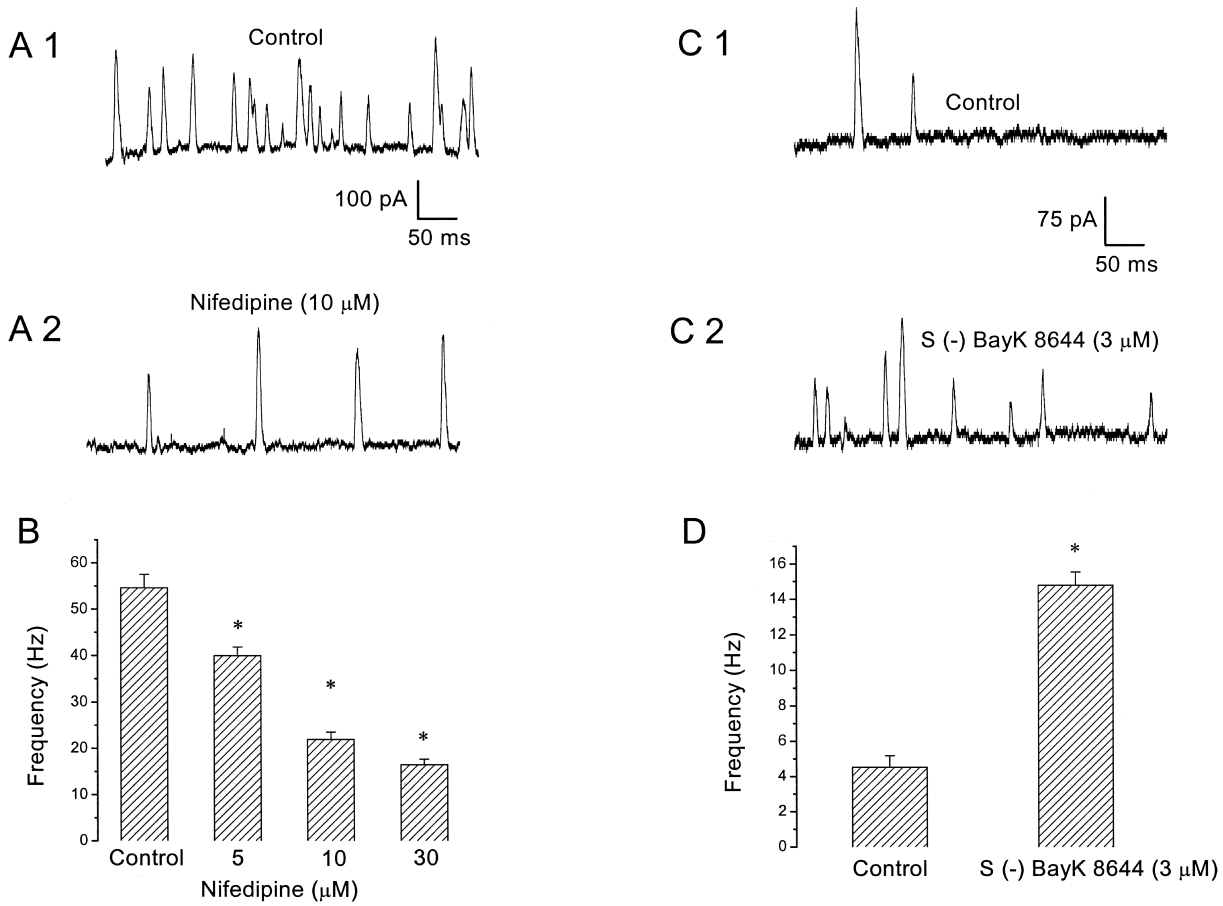

FIGURE 4. Dihydropyridine-sensitive VGCCs are involved in SMOC generation. (A) SMOCs were elicited with voltage steps to −10 mV in 6 mM Co^{2+}/1.8 mM Ca^{2+} Ringer's or after addition of 10 μM nifedipine, which decreased SMOC frequency. SMOCs were superimposed on a baseline current of ~95 pA. (B) Nifedipine causes a dose-dependent reduction in SMOC frequency. Data from the same cell as above. Values obtained with each dose of nifedipine were statistically different from control (asterisk indicates $P < 0.01$). (C) S (−) BayK 8644 increased SMOC frequency. SMOCs were generated in 6 mM Co^{2+}/1.8 mM Ca^{2+} Ringer's with a voltage step to −10 mV (C1) or in the presence of 3 μM S (−) BayK 8644 (C2). The baseline current was ~55 pA. (D) Frequency data from the same cell shown in C. S (−) BayK 8644 (3 μM) increased the frequency of SMOC from a control value of 4.5 ± 0.6 Hz to 14.8 ± 0.7 Hz (asterisk indicates $P < 0.01$).

a graded, dose-dependent reduction in SMOC frequency. In this cell, nifedipine reduced SMOC frequency from a control value of 54.6 ± 2.9 Hz to 22 ± 1.6 Hz at 10 μM ($P < 0.01$). However, even at doses of 60 μM, nifedipine was unable to totally block SMOC generation. Average data from seven cells in which SMOCs were recorded under 6 mM Co^{2+}/1.8 mM Ca^{2+} Ringer's at 30 mV gave control frequencies of 20 ± 1.6 Hz, but 8.6 ± 0.6 Hz in 10 μM nifedipine ($P < 0.01$). This effect of nifedipine was partially reversible and was qualitatively confirmed in a total of 18 cells. Addition of S (−) BayK 8644 (3 μM), an L-type Ca^{2+} channel agonist, had the opposite effect. Traces from a representative cell are shown in Fig. 4, C1 (control) and C2 (agonist), for SMOCs generated in 6 mM Co^{2+}/1.8 mM Ca^{2+} Ringer's with a voltage step to −10 mV. Control SMOC frequency in this cell was 4.5 ± 0.6 Hz, and it increased to 14.8 ± 0.7 Hz ($P < 0.01$) on addition of the agonist (Fig. 4 D). Average data from six cells in which SMOCs were recorded under similar conditions gave control frequencies of 7.6 ± 0.8 Hz, but 15.6 ± 1 Hz in S (−) BayK 8644 (3 μM) ($P < 0.01$). Qualitatively similar data were recorded from a total of 10 cells. S (−) BayK 8644 at the same dose also enhanced the frequency of SMOCs generated in normal Ringer's at −50 mV ($n = 3$; unpublished data). The effect of the agonist was not reversible. The lack of reversibility of DHP agents has been noted in earlier studies and is probably due to their lipid solubility and uptake into membranes (Pang and Sperelakis, 1984; Nerbonne and Gurney, 1987). The reduction of SMOC frequency by nifedipine and enhancement by S (−) Bay K 8644 strongly suggest that L-type HVA Ca^{2+} channels play a role in SMOC generation. However, the lack of a complete block by high doses of nifedipine leaves open the question of whether this is the only subtype of HVA Ca^{2+} channels involved. Although there is a possibility that other VGCC subtypes, such as N, P, Q, and R, may participate in this process (Bean, 1989; Zhang et al., 1993; Dunlap et al., 1995), a pharmacological examination of the influence of these other Ca^{2+} channels on SMOC frequency was not performed.

SMOCs Are K^+ Currents: Ion Substitution Experiments

In muscle cells, spontaneous inward Cl^- fluxes have also been reported, termed spontaneous transient inward currents (STICs) (Wang et al., 1992; Janssen and Sims, 1994; Henmi et al., 1996). Experiments to determine the ion selectivity of spontaneous events in retinal neurons are summarized in Fig. 5. E_K was varied while E_{Cl} was kept constant by equimolar substitution of NaCl by KCl. Fig. 5 A shows representative SMOCs with 2.5 mM $[K^+]_{ext}$ and with 25 mM $[K^+]_{ext}$ at 20 mV in 6 mM Co^{2+}/1.8 mM Ca^{2+} Ringer's. The mean SMOC amplitude in this cell was 78 ± 4 pA in 2.5 mM $[K^+]_{ext}$, and 36 ± 1 pA

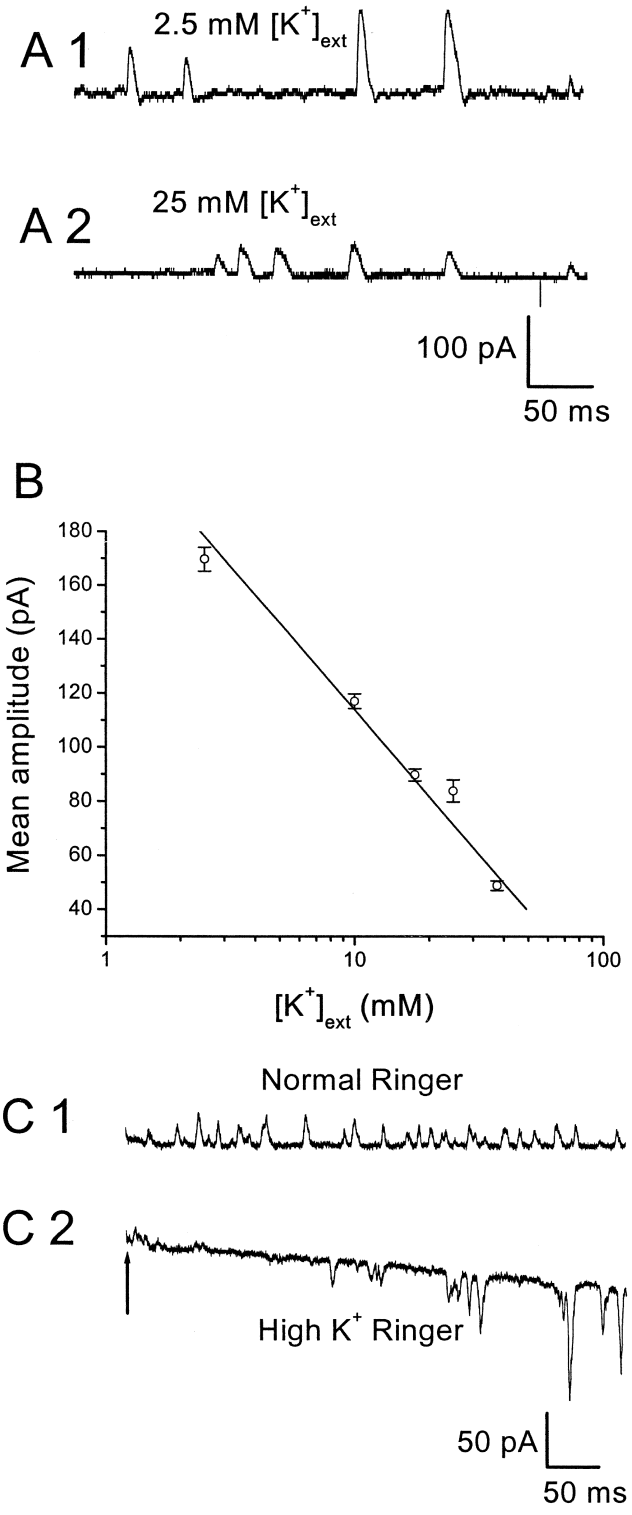

FIGURE 5. SMOCs are K^+ currents based on ion substitution experiments. (A) SMOC amplitude decreases with increase in $[K^+]_{ext}$. SMOCs were generated at 20 mV in 6 mM Co^{2+}/1.8 mM Ca^{2+} Ringer's containing 2.5 mM $[K^+]_{ext}$ (A1). Increasing the $[K^+]_{ext}$ to 25 mM lowered SMOCs amplitudes (A2). SMOCs in A1 were superimposed on a baseline current of 120 pA, and those in A2 on a current of 75 pA. (B) Average data from four cells in which SMOCs were generated at −10 mV by the addition of 6 mM Co^{2+}/1.8 mM Ca^{2+} Ringer's with various K^+ concentrations. The solid line is a lin-

in 25 mM $[K^+]_{ext}$. Mean SMOC amplitude decreased as the $[K^+]_{ext}$ increased. Fig. 5 B plots mean SMOC amplitude versus log $[K^+]_{ext}$. The data points are average values obtained from four cells in which SMOCs were generated at −10 mV by the addition of 6 mM Co^{2+}/1.8 mM Ca^{2+} Ringer's with various K^+ concentrations. SMOCs had mean amplitudes (in pA) of 169.69 ± 4.4 (2.5 mM $[K^+]_{ext}$), 117.01 ± 2.7 (10 mM $[K^+]_{ext}$), 89.79 ± 2.2 (17.5 mM $[K^+]_{ext}$), 83.86 ± 4 (25 mM $[K^+]_{ext}$), and 48.92 ± 1.8 (37.5 mM $[K^+]_{ext}$). A linear fit provides a slope of −106.69 under these conditions; corresponding to an average conductance of 1830 pS or ~16 BK channels at the peak of the SMOC (see DISCUSSION).

SMOCs generated in normal Ringer's at −55 mV could be made to reverse direction by increasing $[K]_{ext}$ to 110 mM (high K^+ Ringer's; $n = 4$). In three out of the four cells tested, switching to high K^+ Ringer's resulted in a large holding current and an eventual obscuring of SMOCs at this negative voltage. Although the cause for this is not clear, it is most likely due to an enhancement of the resting K^+ leak conductance. Moreover, the elicited sustained K^+ currents showed a marked slowing of deactivation under such conditions, which additionally contributed to this effect (Swenson and Armstrong, 1981). Nevertheless, SMOCs were observed to reverse direction immediately after switching to the high K^+ Ringer's. This is shown in Fig. 5 C. The arrow in Fig. 5 C2 marks the point at which the solution change was started. The baseline current gradually increased and SMOCs became inward. The effects of high K^+ Ringer's were fully reversible. These ion substitution studies suggest that retinal SMOCs are primarily K^+ currents.

SMOCs Are K^+ Currents: Pharmacological Block

SMOCs recorded in Co^{2+}-containing solutions were blocked completely by the K^+ channel blocker, TEA (10 mM; $n = 10$). Representative traces showing TEA block of SMOCs generated at −10 mV in 6 mM Co^{2+}/1.8 mM Ca^{2+} Ringer's are shown in Fig. 6 A. The TEA block was fully reversible. Increasing concentrations of TEA produced a graded reduction of SMOC amplitude at −10 mV in 6 mM Co^{2+}/1.8 mM Ca^{2+} Ringer's (Fig. 6 B). In this cell, SMOCs had a mean amplitude of 159 ± 3 pA under control conditions and 91 ± 2 pA in the presence of 0.5 mM TEA. Average SMOC data from four cells under similar conditions gave control amplitudes of 204.9 ± 6.4 pA, and 108.4 ± 3.1 pA in 500 μM TEA (a reduction of ~47%; $P < 0.01$). TEA also produced a dose-dependent decline in SMOC frequency (unpublished data). This is probably due to reduction in amplitude by TEA, causing SMOCs of smaller amplitude to merge with the baseline noise and escape detection. SMOCs generated in normal Ringer's at −50 mV were also blocked by 10 mM TEA ($n = 4$). SMOCs were not blocked by 5 mM 4-aminopyridine (4-AP; $n = 9$). Prolonged exposure (>2 min, as compared with a perfusion equilibration time with an upper limit of 10 s) to 4-AP resulted in a gradual, irreversible decline in SMOC frequency and subsequent elimination of SMOCs. This was not reversible on returning to control. However, SMOCs could be reinstated after pulsing to depolarized levels in normal Ringer's, a process that presumably permits Ca^{2+} influx into the cell and replenishes stores. This effect of prolonged 4-AP application may be nonspecific. It is reminiscent of a gradual rundown/depletion phenomena, probably arising from effects of 4-AP on other molecules, such as the Ca^{2+} ATPases (Ishida and Honda, 1993). The significant blockade of SMOCs by submillimolar amounts of TEA further substantiates that SMOCs are currents generated via fluxes through K^+ channels.

SMOCs Are Currents through Large Conductance Ca^{2+}-activated K^+ Channels (BK Channels)

Fig. 6 C shows that SMOCs generated in 6 mM Co^{2+}/1.8 mM Ca^{2+} Ringer's can be eliminated by the addition of a blocker of BK channels, 100 nM iberiotoxin ($n = 5$, $V_{cmd} = -10$ mV). The onset of iberiotoxin block is relatively slow (2 min) and like TEA, there was a graded reduction in SMOC amplitude and frequency (unpublished data). The block by iberiotoxin was not reversible on switching back to toxin-free control solution.

Since intracellularly stored Ca^{2+} is involved in the SMOC generation pathway, care was taken to ensure that the slow time course and irreversibility of iberiotoxin block was not mistaken for rundown/depletion. Control recordings for 2 min did not show a significant change in SMOC frequency or amplitude. However, addition of 100 nM iberiotoxin led to a total block of SMOCs in the subsequent 2 min. Moreover, contrary to what would be expected for depletion-induced phenomena, refilling of stores by pulsing to depolarized levels in normal Ringer's failed to reinstate SMOCs. This suggested a persistence of iberiotoxin block independent of depletion of the Ca^{2+} store.

Apamin (100 nM), a blocker of small conductance Ca^{2+}-activated K^+ channels (SK channels), did not eliminate SMOCs generated at depolarized levels in 6 mM Co^{2+}/1.8 mM Ca^{2+} Ringer's nor affect their characteristics ($n = 7$; unpublished data). SMOCs generated in normal Ringer's at −50 mV were blocked by 100 nM iberiotoxin, but not by 100 nM apamin ($n = 8$; unpublished data). These results suggest that SMOCs are K^+ fluxes through the BK subtype of K_{Ca} channels.

ear fit to the data. (C) SMOCs generated at −55 mV in normal Ringer's (C1; $E_k = -95$ mV) reversed direction in high K^+ Ringer's (C2; $E_k = 0$ mV). SMOCs were the only observed current in normal Ringer's at this voltage. The arrow in C2 indicates the point at which superfusion of high K^+ Ringer's was started.

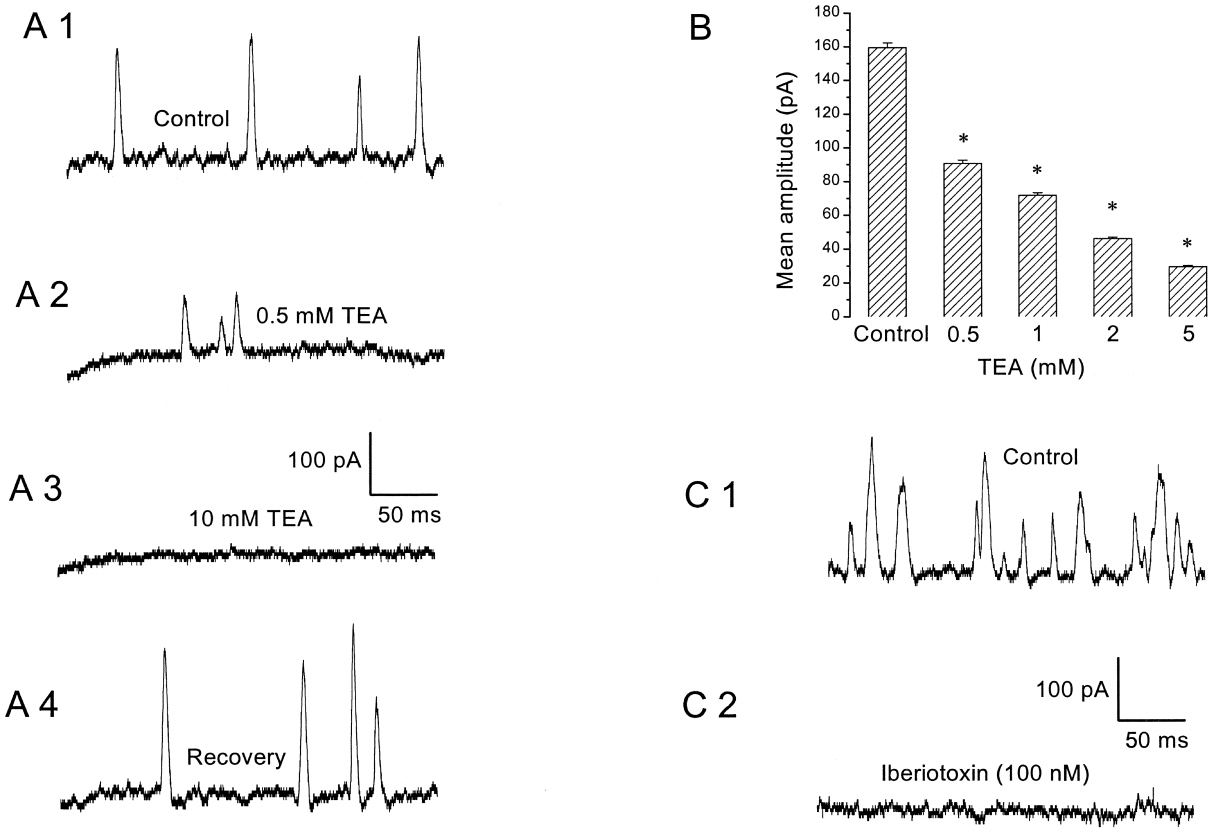

FIGURE 6. Effects of K^+ channel blockers on SMOCs. (A) SMOCs were elicited with voltage steps to −10 mV in 6 mM Co^{2+}/1.8 mM Ca^{2+} Ringer's. Control SMOCs shown in A1 were reduced in amplitude by 0.5 mM TEA (A2). Addition of 10 mM TEA abolished SMOCs (A3). The blockade by TEA was fully reversible on washout of the drug (A4). SMOCs were superimposed on baseline currents of 151 pA (A1), 108 pA (A2), 63 pA (A3), and 155 pA (A4). (B) Effect of increasing doses of TEA on peak SMOC amplitudes. Data obtained from the same cell and values at each dose are significantly lower than control (asterisk indicates $P < 0.01$). (C) Control SMOCs generated at −10 mV in 6 mM Co^{2+}/1.8 mM Ca^{2+} Ringer's to which 0.1% wt/vol BSA was added (C1). Addition of 100 nM iberiotoxin eliminated SMOCs (C2). Baseline current was ~100 pA.

CICR Mediates SMOC Generation

Although the earlier sections showed that Ca^{2+} influx through HVA Ca^{2+} channels plays a role in the generation of SMOCs, there are reports in other neuronal preparations of SMOCs being activated by CICR triggered by Ca^{2+} influx. Ca^{2+} release from internal stores also mediates the generation of STOCs in muscle cells (see INTRODUCTION). Moreover, SMOCs were induced under conditions of inorganic Ca^{2+} channel blockade, where Ca^{2+} influx was severely reduced. Under such conditions an internal amplification mechanism is likely to exist. To test this possibility, we internally dialyzed neurons with ryanodine, a plant alkaloid that blocks RyRs at high doses (Zucchi and Ronca-Testoni, 1997). Internal dialysis of ryanodine (200 μM) abolished SMOCs generated either in normal Ringer's or in Co^{2+}-containing solutions (n = 7). Cells were identified as having the requisite current signature immediately on achieving the whole cell configuration. Control SMOCs were immediately recorded, before sufficient dialysis took place. Fig. 7 A1 shows an example in which control SMOCs were recorded 17 s after achieving the whole cell configuration. These SMOCs were recorded in 6 mM Co^{2+}/1.8 mM Ca^{2+} Ringer's at 30 mV with 200 μM ryanodine added to the internal pipette solution. Dialysis of the neuron for a further 35 s led to the total elimination of SMOCs (Fig. 7 A2).

The methylxanthine, caffeine, is known to sensitize the ryanodine receptor Ca^{2+} release channel, such that CICR occurs in response to much lower levels of $[Ca^{2+}]_i$. Even resting levels of $[Ca^{2+}]_i$ are sufficient to cause CICR in the presence of caffeine (Verkhratsky and Shmigol, 1996). Thus, high doses of caffeine (10 mM) deplete stored Ca^{2+} within cells. Consequently, any process dependent on CICR for its activation should be eliminated and not reappear until these stores are replenished. Consistent with this expectation, it was found that 10 mM caffeine eliminated SMOCs generated either in normal Ringer's or in the presence of inorganic blockers (n = 17). Fig. 7 B1 shows an example in which SMOCs were generated at −10 mV in the presence of 6 mM Co^{2+}/1.8 mM Ca^{2+} Ringer's. Exposure to 10 mM

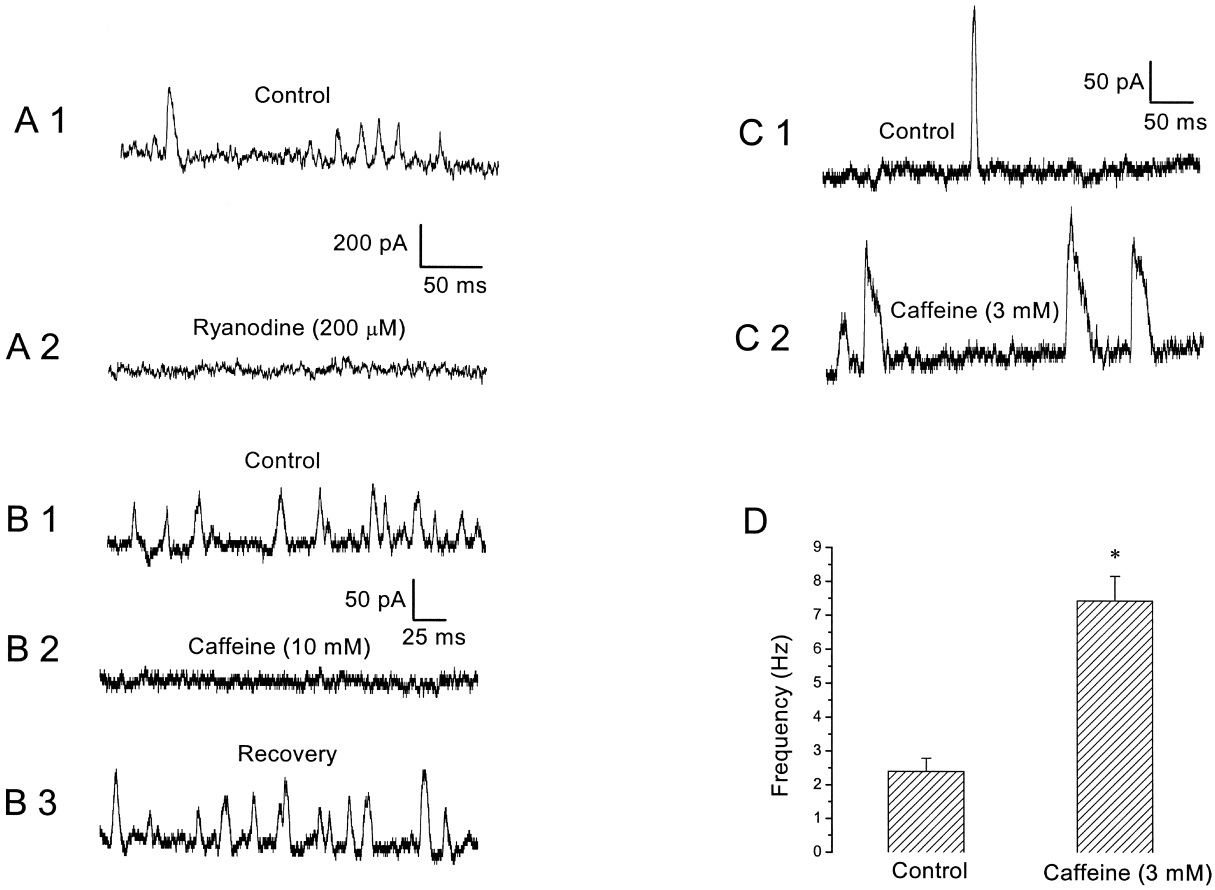

FIGURE 7. CICR mediates SMOC generation. (A) Control SMOCs were recorded at 30 mV in 6 mM Co^{2+}/1.8 mM Ca^{2+} Ringer's ~17 s after achieving the whole cell configuration (A1). Dialysis for a further 35 s with 200 μM ryanodine eliminated SMOC activity (A2). SMOCs in this cell were superimposed on a baseline current of ~1600 pA. (B) Control SMOCs were generated at −10 mV in 6 mM Co^{2+}/1.8 mM Ca^{2+} Ringer's (B1). Addition of 10 mM caffeine eliminated SMOC activity (B2). The SMOC activity could be restored to original frequencies only after pulsing to depolarized levels in normal Ringer's (B3). The baseline current was ~170 pA. (C) Control SMOCs shown in C1 were generated at −10 mV in 6 mM Co^{2+}/0.9 mM Ca^{2+} Ringer's. Transient exposure to 3 mM caffeine enhanced SMOC frequency and broadened individual SMOCs (C2). The baseline current was ~80 pA. (D) Stimulatory effect of 3 mM caffeine on SMOC frequency (average of four cells; asterisk indicates $P < 0.01$).

caffeine completely eliminated SMOCs (Fig. 7 B2). Caffeine is known to have some other nonspecific effects such as blockade of K^+ channels (Reiser et al., 1996). Although this possibility cannot be totally discounted, it is likely that store depletion accounts for SMOC elimination for the following reasons: (a) the baseline K^+ current at −10 mV was not affected by caffeine, whereas SMOCs were eliminated, and (b) it is expected that any block should be relieved on washout of the blocking agent. In contrast, store depletion–induced effects can recover only after replenishment of the stores. Consistent with this, SMOCs did not recover rapidly after washout of caffeine. They could be reinstated to their original frequencies (Fig. 7 B3) only after the cell was switched to normal Ringer's and pulsed repeatedly to 30 mV to replenish the internal calcium stores. This necessity for pulsing to depolarized levels to recover the original SMOC activity after caffeine treatment was most apparent in three cells in which SMOCs were generated in normal Ringer's at −50 mV. Based on evidence in other neurons, it is proposed that pulsing to depolarized levels in normal Ringer's activated the HVA Ca^{2+} channels, resulting in a substantial Ca^{2+} influx into the cell, which eventually led to store replenishment (Brorson et al., 1991; Friel and Tsien, 1992; Shmigol et al., 1994; Garaschuk et al., 1997). In contrast to other neurons displaying SMOCs, we did not observe that high doses of caffeine induced an outward current (Merriam et al., 1999; Arima et al., 2001).

Although prolonged exposure to high doses of caffeine causes store depletion, caffeine should initially be able to stimulate CICR and augment any process dependent on it. This was verified by exposing cells transiently to low doses of caffeine (1–3 mM). In a representative cell, control SMOCs were generated in 6 mM Co^{2+}/0.9 mM Ca^{2+} Ringer's at −10 mV (Fig. 7 C1). Exposure to 3 mM caffeine increased SMOC frequency (Fig. 7 C2). In a set of four cells, mean SMOC fre-

quency under control conditions was 2.4 ± 0.4 Hz, but on exposure to 3 mM caffeine SMOC frequency increased to 7.4 ± 0.7 Hz (Fig. 7 D, $P < 0.01$).

A comparison of Fig. 7 C2 with C1 shows that 3 mM caffeine also increased SMOC decay time. The mean 50% decay time ($t_{1/2}$) of control SMOCs in 6 mM Co^{2+}/0.9 mM Ca^{2+} Ringer's at −10 mV was 3.2 ± 0.2 ms, whereas caffeine-induced SMOCs had a $t_{1/2}$ of 8.7 ± 0.4 ms (four cells, $P < 0.01$). Combined with the earlier finding that Ca^{2+} influx is a prerequisite for SMOC generation, these experiments with caffeine and ryanodine argue in favor of a RyR-mediated CICR in the process of SMOC generation.

SMOC Activity Is Eliminated by Intracellular Ca^{2+} Chelation with BAPTA but not by EGTA

As expected for any $[Ca^{2+}]_i$-dependent process, intracellular Ca^{2+} chelators have been shown to eliminate both STOCs and SMOCs (Benham and Bolton, 1986; Bychkov et al., 1997; Merriam et al., 1999). Since CICR was shown to be involved in the SMOC generation pathway in retinal neurons, the effect of internal Ca^{2+} chelators was tested. The affinities of both BAPTA and EGTA for Ca^{2+} are similar, although BAPTA is known to have an association rate that is ~150 times greater as compared with EGTA (Naraghi, 1997). Thus, contrasting the effects of these two chelators would allow distinction between fast and slow Ca^{2+}-stimulated events over short distances. BAPTA eliminated SMOCs generated either in normal Ringer's or Co^{2+}-containing solutions. An example is shown in Fig. 8 A, in which SMOCs were recorded 30 s after achieving the whole cell configuration at 30 mV in 6 mM Co^{2+}/1.8 mM Ca^{2+} Ringer's with 10 mM BAPTA in the internal solution. Dialysis of the neuron for a subsequent 46 s totally eliminated SMOCs (Fig. 8 A2). This result was confirmed in 13 cells. EGTA did not have any effect on SMOC activity even on prolonged dialysis ($n = 5$). Data from a representative cell is shown in Fig. 8 B, where control SMOCs were recorded 2 min after achieving the whole cell configuration (Fig. 8 B1). Continued dialysis for another 5 min had no effect on SMOC activity (Fig. 8 B2). These results suggest a local, rapid increase in $[Ca^{2+}]_i$ is responsible for generation of SMOCs.

DISCUSSION

This study identifies a novel current, SMOCs, hitherto unidentified in the retina. In normal Ringer's, SMOCs were observed in a subset of amacrine cells within a narrow voltage window of −60 to −40 mV. They were random, spike-shaped and TTX-insensitive, with similarity to currents reported in other neuronal types (Mathers and Barker, 1981, 1984; Satin and Adams, 1987; Merriam et al., 1999; Arima et al., 2001; Scornik et al., 2001).

SMOCs observed in these experiments, whether in Ringer's or Co^{2+}-containing solutions, were induced with voltage pulses and thus strictly speaking were not "spontaneous." However, the term "SMOCs" has been employed to maintain consistency with literature on similar phenomena in other neuronal types. Moreover, the isolated cell preparation does not allow determination of the normal resting potential. In situ, these amacrine cells may rest within the voltage range where SMOCs occur. Alternatively, these neurons may rest at more negative potentials but SMOCs could be "evoked" by small depolarizing shifts caused by spon-

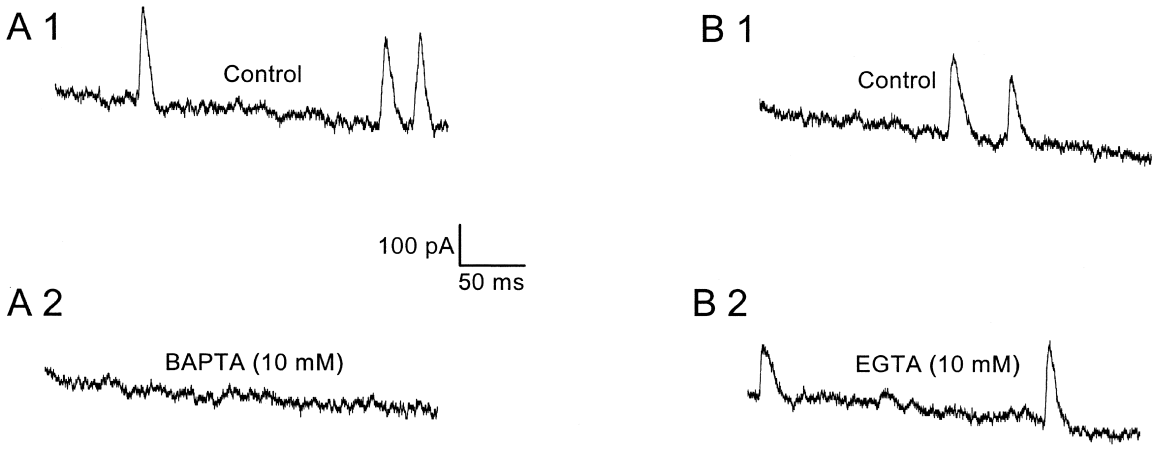

FIGURE 8. SMOC activity was eliminated by BAPTA but not by EGTA. SMOCs were generated at 30 mV in 6 mM Co^{2+}/1.8 mM Ca^{2+} Ringer's. The recording pipette contained 10 mM BAPTA (A) or 10 mM EGTA (B). (A) Control SMOCs shown in A1 were recorded 30 s after achieving the whole cell configuration. Dialysis for a further 46 s led to elimination of SMOC activity (A2). (B) Control SMOCs shown in B1 were recorded 2 min after achieving the whole cell configuration. Dialysis of the neuron for a further 5 min had no effect on SMOC activity (B2). The sag in the traces is presumably due to inactivation of voltage-dependent potassium channels. SMOCs in A were superimposed on a baseline current that peaked at 1295 pA and decayed to 900 pA at the end of the 500 ms pulse, whereas those in B were superimposed on a current peaking at 1540 pA and decayed to 1155 pA at the end of 500 ms.

taneous miniature excitatory postsynaptic currents (sEPSCs).

In these amacrine cells, depolarizing shifts in voltage elicit a successive series of outward currents: SMOCs, I_{to}, and I_{so}. The I_{so} can be further decomposed into $I_{so\text{-}Ca}$ and a purely voltage-dependent $I_{so\text{-}v}$. Except for the $I_{so\text{-}v}$, the other three outward currents are Ca^{2+}-sensitive. It is shown in the following paper that iberiotoxin not only eliminates SMOCs and the I_{to}, it also reduces the I_{so}. However, depletion of the internal stores with caffeine eliminates SMOCs and the I_{to}, but does not affect the I_{so} (Mitra and Slaughter, 2002, this issue). Thus, all three outward currents have components generated by BK channels, the distinction being that $I_{so\text{-}Ca}$ is not activated by CICR.

Properties of the Sustained Outward Current

The I_{so} appeared at −30 mV and increased linearly with depolarization. It consisted of calcium-dependent ($I_{so\text{-}Ca}$) and calcium-independent ($I_{so\text{-}v}$) components. $I_{so\text{-}v}$ activated and then increased linearly with depolarization. $I_{so\text{-}Ca}$ activated at slightly more negative potentials, but showed a decline at positive voltages. When the contribution of $I_{so\text{-}Ca}$ and $I_{so\text{-}V}$ to total I_{so} is considered, the percentage of $I_{so\text{-}v}$ increased with depolarizations and that of the $I_{so\text{-}Ca}$ decreased. This decline of the $I_{so\text{-}Ca}$ fraction may be due to the decline in Ca^{2+} influx with depolarization. It is known that K_{Ca} channels (BK subtype) are activated by concerted influences of both $[Ca^{2+}]_i$ and voltage. Their sensitivity to Ca^{2+} increases with membrane depolarization (Barrett et al., 1982; Vergara et al., 1998). Therefore, the decline of the $I_{so\text{-}Ca}$ fraction with depolarization reflects the interaction between the activation-favoring effects of depolarized potentials and the activation-reducing effects of lowered Ca^{2+} influx at those voltages.

SMOC Properties

Our results indicate that SMOCs are transient K^+ fluxes through plasmalemmal BK channels and originate from Ca^{2+} influx through VGCCs; this influx being amplified by CICR from caffeine- and ryanodine-sensitive intracellular stores. Earlier studies in smooth muscle reported STOCs, which are similar to SMOCs (Benham and Bolton, 1986; Bolton and Imaizumi, 1996). Although similar, neuronal SMOCs are more transient than smooth muscle STOCs (Merriam et al., 1999). Retinal SMOCs show an interevent interval distribution that is exponential, characteristic of stochastic events (Fatt and Katz, 1952; Hubbard et al., 1969). This is in agreement with reports of randomly occurring SMOCs in cultured bullfrog neurons (Satin and Adams, 1987).

In smooth muscle, spontaneous activation of potassium or chloride channels produce currents of opposite polarity. Thus, smooth muscle exhibits STOCs when discrete release of Ca^{2+} from internal stores activates potassium channels, and STICs when the same processes activate chloride channels (Wang et al., 1992; Janssen and Sims, 1994; Henmi et al., 1996). But in neurons, either conductance will produce an outward current. Retinal SMOCs are K^+ currents, since their mean amplitude varied with the $[K^+]_{ext}$ in a Nernstian manner. Since they are blocked by iberiotoxin and insensitive to apamin, they likely represent openings of clusters of BK channels (McManus, 1991; Kaczorowski et al., 1996). Extracellular TEA, which decreases the amplitude of single channel currents through BK channels in a concentration-dependent manner (Saunders and Farley, 1992), reduced retinal SMOC amplitudes in a dose-dependent manner, eliminating them at 10 mM. These findings concur with published data on both STOCs and SMOCs in other cell types, which show them to be coordinated openings of K_{Ca} channels of the BK subtype (Bolton and Imaizumi, 1996; Merriam et al., 1999). However, small conductance K_{Ca} (SK subtype) channels can also generate SMOCs, as shown in rat Meynert neurons (Arima et al., 2001).

Retinal SMOCs generated at −50 mV in normal Ringer's displayed a mean amplitude of 33 ± 0.5 pA. BK channels have been reported to have conductances in the range of 115–118 pS in third order neurons in mammalian retina (Lipton and Tauck, 1987; Wang et al., 1998). Assuming a similar conductance in amphibian neurons, it is estimated that retinal SMOCs generated in normal Ringer's represent an average opening of ~6 BK channels at their peak. The maximum SMOC height seen in normal Ringer's at this voltage was 92 pA, which would represent the opening of ~18 BK channels. SMOCs generated in 6 mM Co^{2+}/1.8 mM Ca^{2+} Ringer's at −10 mV had a mean amplitude of 158 ± 3 pA corresponding to ~16 BK channels. The slope of the fitted data shown in Fig. 5 B gives a similar estimate. Fletcher and Chiappinelli (1992) examined spontaneous miniature hyperpolarizations (SMHs; the voltage equivalent of SMOCs) in chick ciliary ganglion neurons and reported ~15–60 channels in each SMH, whereas Scornik et al. (2001) in mudpuppy cardiac neurons arrived at a value of 18–23 channels in the average SMOC. SMOCs in retinal neurons are similar to these reports, rather than bullfrog sympathetic neurons wherein each SMOC was reported to constitute activation of 10–5,000 channels (Satin and Adams, 1987). In spite of the small number of channels, single channel currents were not observed. Perhaps the recording bandwidth led to the filtering of such single steps.

Voltage-gated Calcium Channels Initiate SMOCs

The Ca^{2+} ions necessary for the activation of K_{Ca} channels can be provided either via extracellular influx or release from intracellular stores (Zorumski et al., 1989;

Wisgirda and Dryer, 1994; Davies et al., 1996; Marrion and Tavalin, 1998; Hurley et al., 1999; Imaizumi et al., 1999). Satin and Adams (1987), in their study of SMOCs in bullfrog sympathetic neurons, reported that Ca^{2+} influx through surface membrane Ca^{2+} channels was not essential for SMOC generation. They suggested that neuronal depolarization directly coupled to Ca^{2+} release from internal stores. Their conclusions were based on the finding that 100 μM Cd^{2+} did not block SMOCs. Fletcher and Chiappinelli (1992) found a similar insensitivity to external Ca^{2+} in chick ciliary ganglion neurons. Arima et al. (2001) suggest that Ca^{2+} influx contributes to, but is not essential, for SMOC generation in rat Meynert neurons. However, other investigators found Ca^{2+} influx was required for SMOC generation (Mathers and Barker, 1981, 1984; Merriam et al., 1999). Retinal SMOCs were instantly eliminated when cells were exposed to nominal [Ca^{2+}] containing solutions, and immediately recovered when bath Ca^{2+} was reinstated.

Retinal SMOCs were initiated by Ca^{2+} influx through plasmalemmal VGCCs. SMOCs are seen in normal Ringer's at membrane potentials between −60 to −40 mV. Addition of inorganic VGCC blockers such as Co^{2+} or Cd^{2+} eliminated SMOCs at these hyperpolarized levels, although they reappeared at more depolarized voltages, at or above −20 mV. It is generally thought that these divalent cations are VGCC pore blockers (Lansman et al., 1986; Winegar et al., 1991). Therefore, depolarization would tend to push the blocker out of the channel and thus relieve block (Woodhull, 1973; Fukushima and Hagiwara, 1985; Thevenod and Jones, 1992; Carbone et al., 1997; Wakamori et al., 1998). Increasing the dose of the inorganic blocker resulted in a graded reduction in retinal SMOC frequency. Stimulating non-VGCC–mediated Ca^{2+} influx by activation of kainic acid receptors did not affect SMOC frequency. These observations suggested that Ca^{2+} influx through VGCCs is necessary for SMOC generation.

DHPs are a group of Ca^{2+} channel ligands that are thought to be selective for the L-type HVA Ca^{2+} channel (Bean, 1984; Nowycky et al., 1985; Fox et al., 1987; Rane et al., 1987). L-type HVA Ca^{2+} channels are known to be in close proximity to the RyRs in cardiac muscle, and it is presumably this anatomical arrangement that enables the occurrence of discrete Ca^{2+} release events called "sparks" (Carl et al., 1995; Sun et al., 1995). In smooth muscle cells, sparks have been implicated as the underlying event giving rise to STOCs (Nelson et al., 1995; Mironneau et al., 1996; Perez et al., 1999; ZhuGe et al., 1999). A similar anatomical relationship may also exist in smooth muscle cells (Jaggar et al., 1998). Our experiments revealed the involvement of L-type HVA Ca^{2+} channels in retinal SMOC generation. The DHP blocker, nifedipine, reduced SMOC frequency in a dose-dependent manner and the agonist S (−) BayK 8644 increased it. Although nifedipine reduced SMOC frequency, it never completely eliminated SMOCs, even at concentrations up to 60 μM at relatively depolarized voltage of 30 mV. This result may be interpreted in two ways. One is that other subtypes of HVA calcium channel, such as N, P, Q, and R, may be involved (Bean, 1989; Zhang et al., 1993; Dunlap et al., 1995), and that the system does not show any specificity as regards the type of HVA Ca^{2+} channel that generates SMOCs. This was the conclusion arrived at by Merriam et al. (1999) in their study of SMOCs in mudpuppy parasympathetic cardiac neurons. The involvement of other subtypes of HVA Ca^{2+} channels was not examined in this present study. The alternative explanation is that the L-type VGCCs are not totally blocked, even with high doses of nifedipine, and the consequent high amplification of the trigger Ca^{2+} signal by CICR leads to a SMOC. Blockade by DHP antagonists is complex since cell voltage affects it. These blockers have a higher affinity for the inactivated state of the channel, the population of which increases as the cell is depolarized (Bean, 1984; Sanguinetti and Kass, 1984). It may be that this voltage dependence of nifedipine block does not allow a 100% block even at depolarized voltages, permitting a stochastic unblock of a few Ca^{2+} channels. It has been shown in heart muscle that influx through one Ca^{2+} channel is enough to activate CICR (Santana et al., 1996). This would be all the more likely if the intracellular stores are filled with Ca^{2+}, since it has been shown that store filling increases the sensitivity of the stores to generate CICR, whereas store depletion has the opposite effect (Friel and Tsien, 1992; Jaffe and Brown, 1994; Shmigol et al., 1996; Hernandez-Cruz et al., 1997; Usachev and Thayer, 1997). Although demonstrating the involvement of L-type Ca^{2+} channels in the SMOC generation pathway, this study does not eliminate the involvement of other HVA types.

Calcium-induced Calcium Release Produces SMOCS

Ca^{2+} influx through VGCCs can either directly activate the K_{Ca} channels responsible for SMOCs, or trigger CICR (Sah and McLachlan, 1991; Sah, 1992; Jobling et al., 1993; Berridge, 1998). CICR-triggered via Ca^{2+} influx through VGCCs is the accepted mechanism of Ca^{2+} spark generation in cardiac muscle (Imaizumi et al., 1999). In neurons, CICR has been shown to be an intermediate step for SMOC generation (Mathers and Barker, 1981, 1984; Merriam et al., 1999). In retinal neurons, the effects of both caffeine and ryanodine indicate that CICR is involved in SMOC generation. Low concentrations of ryanodine (<10 μM) lock the release channel in a subconductance state, which is 40–60% of the normal conductance. Higher concentrations (>100 μM) of ryanodine block the release channel in a use-dependent manner (Sutko and Airey, 1996;

Zucchi and Ronca-Testoni, 1997). Caffeine, on the other hand, increases the sensitivity of the channel to trigger Ca^{2+} release, causing significant release even at resting levels of $[Ca^{2+}]_i$ (Verkhratsky and Shmigol, 1996). It increases the open probability of the release channel by generating more frequent openings, whereas the mean open time and conductance is not altered (Rousseau et al., 1988; Rousseau and Meissner, 1989; Sitsapesan and Williams, 1990; Hernandez-Cruz et al., 1995). High doses of caffeine (10 mM) deplete the internal Ca^{2+} stores and thus eliminate CICR (Friel and Tsien, 1992). Low doses of caffeine (1–3 mM) have been shown to augment CICR-dependent process by causing additional Ca^{2+} release in response to the trigger signal. Internal dialysis with 200 μM ryanodine completely eliminated retinal SMOCs. Exposure to 10 mM caffeine eliminated retinal SMOCs, which recovered only after store refilling. Caffeine at low doses (1–3 mM) increased SMOC frequency. Similar effects of low doses of caffeine have been observed on both STOCs and SMOCs (Bolton and Imaizumi, 1996; Merriam et al., 1999; Arima et al., 2001). Retinal SMOCs induced by 1–3 mM caffeine showed a prolonged decay time. Merriam et al. (1999) made a similar observation in mudpuppy parasympathetic neurons, suggesting this reflected caffeine's ability to cause the release channel to open more frequently. As a consequence, there are multiple activations of the BK channels in the vicinity of the release channel, slowing the rate of decay.

Internal BAPTA eliminated SMOC activity, whereas EGTA did not. BAPTA and EGTA have similar affinities for Ca^{2+}, but the former has faster association kinetics (Naraghi, 1997). Consequently, BAPTA can eliminate rises of $[Ca^{2+}]_i$ within more restricted microdomains (Deisseroth et al., 1996; Sham, 1997; Neher, 1998). This differential effect of the two buffers suggests that the $[Ca^{2+}]_i$ rise responsible for activating the BK channels is a highly localized event. A similar observation was reported by Merriam et al. (1999) in mudpuppy cardiac neurons. Such localized $[Ca^{2+}]_i$ elevations, "Ca^{2+} sparks," have been noted in cardiac and smooth muscle (Imaizumi et al., 1999). Based on these findings and the mechanism known to exist in smooth muscle, it would be a reasonable conjecture that a "Ca^{2+} spark" underlies SMOC generation in retinal neurons.

In summary, our experiments show that, in a subset of retinal amacrine cells, Ca^{2+} influx through L-type HVA Ca^{2+} channels triggers CICR from caffeine and ryanodine-sensitive stores. This amplified Ca^{2+} signal subsequently activates clusters of BK channels leading to outward K^+ current fluxes which appear as SMOCs. However, there is a complex relationship between Ca^{2+} influx and SMOC appearance. Although Ca^{2+} influx was found to be a prerequisite for SMOC generation, reducing Ca^{2+} influx caused SMOCs to appear at depolarized voltages while eliminating them at hyperpolarized levels. This would suggest that large amounts of Ca^{2+} influx probably has a negative modulatory effect on SMOCs, since the open probability of VGCCs is usually higher at depolarized voltages. This is addressed in the subsequent paper, which characterizes the biophysical properties of SMOCs, including their Ca^{2+} dependence, and thus provides an explanation for their disappearance at depolarized voltage levels in normal Ringer's. These findings suggest that SMOCs putatively serve to suppress spontaneous excitatory synaptic events within the retinal network (Mitra and Slaughter, 2002, this issue).

The authors wish to thank Drs. Wen Shen and Gautam Awatramani for their valuable input and active help during the course of this work.

This work was supported by NEI grant EY05725. P. Mitra was a recipient of the Mark Diamond Research Fund award for the year 1999–2000.

Submitted: 30 July 2001
Revised: 18 March 2002
Accepted: 19 March 2002

REFERENCES

Arima, J., N. Matsumoto, K. Kishimoto, and N. Akaike. 2001. Spontaneous miniature outward currents in mechanically dissociated rat Meynert neurons. *J. Physiol.* 534:99–107.

Bader, C.R., P.R. MacLeish, and E.A. Schwartz. 1979. A voltage-clamp study of the light response in solitary rods of the tiger salamander. *J. Physiol.* 296:1–26.

Barnes, S., and F. Werblin. 1986. Gated currents generate single spike activity in amacrine cells of the tiger salamander retina. *Proc. Natl. Acad. Sci. USA.* 83:1509–1512.

Barrett, J.N., K.L. Magleby, and B.S. Pallotta. 1982. Properties of single calcium-activated potassium channels in cultured rat muscle. *J. Physiol.* 331:211–230.

Bean, B.P. 1984. Nitrendipine block of cardiac calcium channels: high-affinity binding to the inactivated state. *Proc. Natl. Acad. Sci. USA.* 81:6388–6392.

Bean, B.P. 1989. Classes of calcium channels in vertebrate cells. *Annu. Rev. Physiol.* 51:367–384.

Benham, C.D., and T.B. Bolton. 1986. Spontaneous transient outward currents in single visceral and vascular smooth muscle cells of the rabbit. *J. Physiol.* 381:385–406.

Berridge, M.J. 1993. Inositol trisphosphate and calcium signalling. *Nature.* 361:315–325.

Berridge, M.J. 1998. Neuronal calcium signaling. *Neuron.* 21:13–26.

Betz, H. 1990. Ligand-gated ion channels in the brain: the amino acid receptor superfamily. *Neuron.* 5:383–392.

Bolton, T.B., and Y. Imaizumi. 1996. Spontaneous transient outward currents in smooth muscle cells. *Cell Calcium.* 20:141–152.

Brorson, J.R., D. Bleakman, P.S. Chard, and R.J. Miller. 1992. Calcium directly permeates kainate/alpha-amino-3-hydroxy-5-methyl-4-isoxazolepropionic acid receptors in cultured cerebellar Purkinje neurons. *Mol. Pharmacol.* 41:603–608.

Brorson, J.R., D. Bleakman, S.J. Gibbons, and R.J. Miller. 1991. The properties of intracellular calcium stores in cultured rat cerebellar neurons. *J. Neurosci.* 11:4024–4043.

Bychkov, R., M. Gollasch, C. Ried, F.C. Luft, and H. Haller. 1997. Regulation of spontaneous transient outward potassium currents in human coronary arteries. *Circulation.* 95:503–510.

Carbone, E., H.D. Lux, V. Carabelli, G. Aicardi, and H. Zucker. 1997. Ca^{2+} and Na^{+} permeability of high-threshold Ca^{2+} channels and their voltage-dependent block by Mg^{2+} ions in chick sensory neurones. *J. Physiol.* 504:1–15.

Carl, S.L., K. Felix, A.H. Caswell, N.R. Brandt, W.J. Ball, Jr., P.L. Vaghy, G. Meissner, and D.G. Ferguson. 1995. Immunolocalization of sarcolemmal dihydropyridine receptor and sarcoplasmic reticular triadin and ryanodine receptor in rabbit ventricle and atrium. *J. Cell Biol.* 129:672–682.

Cheng, H., M.R. Lederer, R.P. Xiao, A.M. Gomez, Y.Y. Zhou, B. Ziman, H. Spurgeon, E.G. Lakatta, and W.J. Lederer. 1996. Excitation-contraction coupling in heart: new insights from Ca^{2+} sparks. *Cell Calcium.* 20:129–140.

Cohen, A.S., K.A. Moore, R. Bangalore, M.S. Jafri, D. Weinreich, and J.P. Kao. 1997. Ca^{2+}-induced Ca^{2+} release mediates Ca^{2+} transients evoked by single action potentials in rabbit vagal afferent neurones. *J. Physiol.* 499:315–328.

Davies, P.J., D.R. Ireland, and E.M. McLachlan. 1996. Sources of Ca^{2+} for different Ca^{2+}-activated K^{+} conductances in neurones of the rat superior cervical ganglion. *J. Physiol.* 495:353–366.

Deisseroth, K., H. Bito, and R.W. Tsien. 1996. Signaling from synapse to nucleus: postsynaptic CREB phosphorylation during multiple forms of hippocampal synaptic plasticity. *Neuron.* 16:89–101.

Dowling, J.E., and F.S. Werblin. 1969. Organization of retina of the mudpuppy, Necturus maculosus. I. Synaptic structure. *J. Neurophysiol.* 32:315–338.

Dunlap, K., J.I. Luebke, and T.J. Turner. 1995. Exocytotic Ca^{2+} channels in mammalian central neurons. *Trends Neurosci.* 18:89–98.

Eliasof, S., S. Barnes, and F. Werblin. 1987. The interaction of ionic currents mediating single spike activity in retinal amacrine cells of the tiger salamander. *J. Neurosci.* 7:3512–3524.

Fabiato, A. 1983. Calcium-induced release of calcium from the cardiac sarcoplasmic reticulum. *Am. J. Physiol.* 245:C1–C14.

Fatt, P., and B. Katz. 1952. Spontaneous subthreshold activity in motor nerve endings. *J. Physiol.* 117:109–128.

Fletcher, G.H., and V.A. Chiappinelli. 1992. Spontaneous miniature hyperpolarizations of presynaptic nerve terminals in the chick ciliary ganglion. *Brain Res.* 579:165–168.

Fox, A.P., M.C. Nowycky, and R.W. Tsien. 1987. Single-channel recordings of three types of calcium channels in chick sensory neurones. *J. Physiol.* 394:173–200.

Friel, D.D., and R.W. Tsien. 1992. A caffeine and ryanodine sensitive Ca^{2+} store in bullfrog sympathetic neurons modulates the effects of Ca^{2+} entry on $[Ca^{2+}]i$. *J. Physiol.* 450:217–246.

Fukushima, Y., and S. Hagiwara. 1985. Currents carried by monovalent cations through calcium channels in mouse neoplastic B lymphocytes. *J. Physiol.* 358:255–284.

Garaschuk, O., Y. Yaari, and A. Konnerth. 1997. Release and sequestration of calcium by ryanodine-sensitive stores in rat hippocampal neurones. *J. Physiol.* 502:13–30.

Gilbertson, T.A., R. Scobey, and M. Wilson. 1991. Permeation of calcium ions through non-NMDA glutamate channels in retinal bipolar cells. *Science.* 251:1613–1615.

Gordienko, D.V., A.V. Zholos, and T.B. Bolton. 1999. Membrane ion channels as physiological targets for local Ca^{2+} signalling. *J. Microsc.* 196:305–316.

Hamill, O.P., A. Marty, E. Neher, B. Sakmann, and F.J. Sigworth. 1981. Improved patch-clamp techniques for high-resolution current recording from cells and cell-free membrane patches. *Pflügers Arch.* 391:85–100.

Hartzell, H.C., S.W. Kuffler, R. Stickgold, and D. Yoshikami. 1977. Synaptic excitation and inhibition resulting from direct action of acetylcholine on two types of chemoreceptors on individual amphibian parasympathetic neurones. *J. Physiol.* 271:817–846.

Henmi, S., Y. Imaizumi, K. Muraki, and M. Watanabe. 1996. Time course of Ca^{2+}-dependent K^{+} and Cl^{-} currents in single smooth muscle cells of guinea-pig trachea. *Eur. J. Pharmacol.* 306:227–236.

Hernandez-Cruz, A., M. Diaz-Munoz, M. Gomez-Chavarin, R. Canedo-Merino, D.A. Protti, A.L. Escobar, J. Sierralta, and B.A. Suarez-Isla. 1995. Properties of the ryanodine-sensitive release channels that underlie caffeine-induced Ca^{2+} mobilization from intracellular stores in mammalian sympathetic neurons. *Eur. J. Neurosci.* 7:1684–1699.

Hernandez-Cruz, A., A.L. Escobar, and N. Jimenez. 1997. Ca^{2+}-induced Ca^{2+} release phenomena in mammalian sympathetic neurons are critically dependent on the rate of rise of trigger Ca^{2+}. *J. Gen. Physiol.* 109:147–167.

Hille, B. 1992. Ionic Channels in Excitable Membranes. 2nd ed. Sinauer Associates, Inc. Sunderland, MA. 607 pp.

Hubbard, J.I., R. Llinas, and D.M.J. Quastel. 1969. Electrophysiological Analysis of Synaptic Transmission. 1st ed. Williams and Wilkins Co. Baltimore, MD. 372 pp.

Hurley, B.R., H.G. Preiksaitis, and S.M. Sims. 1999. Characterization and regulation of Ca^{2+}-dependent K^{+} channels in human esophageal smooth muscle. *Am. J. Physiol.* 276:G843–G852.

Imaizumi, Y., Y. Ohi, H. Yamamura, S. Ohya, K. Muraki, and M. Watanabe. 1999. Ca^{2+} spark as a regulator of ion channel activity. *Jpn. J. Pharmacol.* 80:1–8.

Imaizumi, Y., Y. Torii, Y. Ohi, N. Nagano, K. Atsuki, H. Yamamura, K. Muraki, M. Watanabe, and T.B. Bolton. 1998. Ca^{2+} images and K^{+} current during depolarization in smooth muscle cells of the guinea-pig vas deferens and urinary bladder. *J. Physiol.* 510:705–719.

Ishida, Y., and H. Honda. 1993. Inhibitory action of 4-aminopyridine on Ca^{2+}-ATPase of the mammalian sarcoplasmic reticulum. *J. Biol. Chem.* 268:4021–4024.

Jacobs, J.M., and T. Meyer. 1997. Control of action potential-induced Ca^{2+} signaling in the soma of hippocampal neurons by Ca^{2+} release from intracellular stores. *J. Neurosci.* 17:4129–4135.

Jaffe, D.B., and T.H. Brown. 1994. Metabotropic glutamate receptor activation induces calcium waves within hippocampal dendrites. *J. Neurophysiol.* 72:471–474.

Jaggar, J.H., G.C. Wellman, T.J. Heppner, V.A. Porter, G.J. Perez, M. Gollasch, T. Kleppisch, M. Rubart, A.S. Stevenson, W.J. Lederer, et al. 1998. Ca^{2+} channels, ryanodine receptors and Ca^{2+}-activated K^{+} channels: a functional unit for regulating arterial tone. *Acta Physiol. Scand.* 164:577–587.

Janssen, L.J., and S.M. Sims. 1994. Spontaneous transient inward currents and rhythmicity in canine and guinea-pig tracheal smooth muscle cells. *Pflugers Arch.* 427:473–480.

Jobling, P., E.M. McLachlan, and P. Sah. 1993. Calcium induced calcium release is involved in the after hyperpolarization in one class of guinea pig sympathetic neurone. *J. Auton. Nerv. Syst.* 42:251–257.

Kaczorowski, G.J., H.G. Knaus, R.J. Leonard, O.B. McManus, and M.L. Garcia. 1996. High-conductance calcium-activated potassium channels; structure, pharmacology, and function. *J. Bioenerg. Biomembr.* 28:255–267.

Kaneko, A. 1970. Physiological and morphological identification of horizontal, bipolar and amacrine cells in goldfish retina. *J. Physiol.* 207:623–633.

Kostyuk, P., and A. Verkhratsky. 1994. Calcium stores in neurons and glia. *Neuroscience.* 63:381–404.

Kuba, K. 1994. Ca^{2+}-induced Ca^{2+} release in neurones. *Jpn. J. Physiol.* 44:613–650.

Lam, D.M.K. 1972. Biosynthesis of acetylcholine in turtle photoreceptors. *Proc. Natl. Acad. Sci. USA.* 69:1987–1991.

Lansman, J.B., P. Hess, and R.W. Tsien. 1986. Blockade of current through single calcium channels by Cd^{2+}, Mg^{2+}, and Ca^{2+}. Voltage and concentration dependence of calcium entry into the pore. *J. Gen. Physiol.* 88:321–347.

Latorre, R., A. Oberhauser, P. Labarca, and O. Alvarez. 1989. Variet-

ies of calcium-activated potassium channels. *Annu. Rev. Physiol.* 51:385–399.

Lipton, S.A., and D.L. Tauck. 1987. Voltage-dependent conductances of solitary ganglion cells dissociated from the rat retina. *J. Physiol.* 385:361–391.

Marrion, N.V., and S.J. Tavalin. 1998. Selective activation of Ca^{2+}-activated K^+ channels by co-localized Ca^{2+} channels in hippocampal neurons. *Nature.* 395:900–905.

Mathers, D.A., and J.L. Barker. 1981. Spontaneous hyperpolarizations at the membrane of cultured mouse dorsal root ganglion cells. *Brain Res.* 211:451–455.

Mathers, D.A., and J.L. Barker. 1984. Spontaneous voltage and current fluctuations in tissue cultured mouse dorsal root ganglion cells. *Brain Res.* 293:35–47.

McManus, O.B. 1991. Calcium-activated potassium channels: regulation by calcium. *J. Bioenerg. Biomembr.* 23:537–560.

Merriam, L.A., F.S. Scornik, and R.L. Parsons. 1999. Ca^{2+}-induced Ca^{2+} release activates spontaneous miniature outward currents (SMOCs) in parasympathetic cardiac neurons. *J. Neurophysiol.* 82: 540–550.

Mironneau, J., S. Arnaudeau, N. Macrez-Lepretre, and F.X. Boittin. 1996. Ca^{2+} sparks and Ca^{2+} waves activate different Ca^{2+}-dependent ion channels in single myocytes from rat portal vein. *Cell Calcium.* 20:153–160.

Mitra, P., and M. Slaughter. 2000. Low calcium influx induced potassium current spikes in retinal third order neurons. *Invest. Ophthalmol. Vis. Sci.* 41:S618.

Mitra, P., and M.M. Slaughter. 2002. Calcium-induced transitions between the spontaneous miniature outward and the transient outward currents in retinal amacrine cells. *J. Gen. Physiol.* 119: 373–388.

Naraghi, M. 1997. T-jump study of calcium binding kinetics of calcium chelators. *Cell Calcium.* 22:255–268.

Narahashi, T., A. Tsunoo, and M. Yoshii. 1987. Characterization of two types of calcium channels in mouse neuroblastoma cells. *J. Physiol.* 383:231–249.

Neher, E. 1998. Vesicle pools and Ca^{2+} microdomains: new tools for understanding their roles in neurotransmitter release. *Neuron.* 20:389–399.

Nelson, M.T., H. Cheng, M. Rubart, L.F. Santana, A.D. Bonev, H.J. Knot, and W.J. Lederer. 1995. Relaxation of arterial smooth muscle by calcium sparks. *Science.* 270:633–637.

Nerbonne, J.M., and A.M. Gurney. 1987. Blockade of Ca^{2+} and K^+ currents in bag cell neurons of Aplysia californica by dihydropyridine Ca^{2+} antagonists. *J. Neurosci.* 7:882–893.

Nowycky, M.C., A.P. Fox, and R.W. Tsien. 1985. Long-opening mode of gating of neuronal calcium channels and its promotion by the dihydropyridine calcium agonist Bay K 8644. *Proc. Natl. Acad. Sci. USA.* 82:2178–2182.

Otori, Y., J.Y. Wei, and C.J. Barnstable. 1998. Neurotoxic effects of low doses of glutamate on purified rat retinal ganglion cells. *Invest. Ophthalmol. Vis. Sci.* 39:972–981.

Pan, Z.H., and M.M. Slaughter. 1995. Comparison of the actions of glycine and related amino acids on isolated third order neurons from the tiger salamander retina. *Neuroscience.* 64:153–164.

Pang, D.C., and N. Sperelakis. 1984. Uptake of calcium antagonistic drugs into muscles as related to their lipid solubilities. *Biochem. Pharmacol.* 33:821–826.

Perez, G.J., A.D. Bonev, J.B. Patlak, and M.T. Nelson. 1999. Functional coupling of ryanodine receptors to KCa channels in smooth muscle cells from rat cerebral arteries. *J. Gen. Physiol.* 113:229–238.

Pozzan, T., R. Rizzuto, P. Volpe, and J. Meldolesi. 1994. Molecular and cellular physiology of intracellular calcium stores. *Physiol. Rev.* 74:595–636.

Rane, S.G., G.G. Holz, and K. Dunlap. 1987. Dihydropyridine inhibition of neuronal calcium current and substance P release. *Pflugers Arch.* 409:361–366.

Reiser, M.A., T. D'Souza, and S.E. Dryer. 1996. Effects of caffeine and 3-isobutyl-1-methylxanthine on voltage-activated potassium currents in vertebrate neurones and secretory cells. *Br. J. Pharmacol.* 118:2145–2151.

Rousseau, E., J. Ladine, Q.Y. Liu, and G. Meissner. 1988. Activation of the Ca^{2+} release channel of skeletal muscle sarcoplasmic reticulum by caffeine and related compounds. *Arch. Biochem. Biophys.* 267:75–86.

Rousseau, E., and G. Meissner. 1989. Single cardiac sarcoplasmic reticulum Ca^{2+}-release channel: activation by caffeine. *Am. J. Physiol.* 256:H328–H333.

Sah, P. 1992. Role of calcium influx and buffering in the kinetics of Ca^{2+}-activated K^+ current in rat vagal motoneurons. *J. Neurophysiol.* 68:2237–2247.

Sah, P., and E.M. McLachlan. 1991. Ca^{2+}-activated K^+ currents underlying the afterhyperpolarization in guinea pig vagal neurons: a role for Ca^{2+}-activated Ca^{2+} release. *Neuron.* 7:257–264.

Sanguinetti, M.C., and R.S. Kass. 1984. Voltage-dependent block of calcium channel current in the calf cardiac Purkinje fiber by dihydropyridine calcium channel antagonists. *Circ. Res.* 55:336–348.

Santana, L.F., H. Cheng, A.M. Gomez, M.B. Cannell, and W.J. Lederer. 1996. Relation between the sarcolemmal Ca^{2+} current and Ca^{2+} sparks and local control theories for cardiac excitation-contraction coupling. *Circ. Res.* 78:166–171.

Satin, L.S., and P.R. Adams. 1987. Spontaneous miniature outward currents in cultured bullfrog neurons. *Brain Res.* 401:331–339.

Saunders, H.H., and J.M. Farley. 1992. Pharmacological properties of potassium currents in swine tracheal smooth muscle. *J. Pharmacol. Exp. Ther.* 260:1038–1044.

Scornik, F.S., L.A. Merriam, and R.L. Parsons. 2001. Number of K(Ca) channels underlying spontaneous miniature outward currents (SMOCs) in mudpuppy cardiac neurons. *J. Neurophysiol.* 85: 54–60.

Sham, J.S. 1997. Ca^{2+} release-induced inactivation of Ca^{2+} current in rat ventricular myocytes: evidence for local Ca^{2+} signalling. *J. Physiol.* 500:285–295.

Shmigol, A., S. Kirischuk, P. Kostyuk, and A. Verkhratsky. 1994. Different properties of caffeine-sensitive Ca^{2+} stores in peripheral and central mammalian neurones. *Pflugers Arch.* 426:174–176.

Shmigol, A., N. Svichar, P. Kostyuk, and A. Verkhratsky. 1996. Gradual caffeine-induced Ca^{2+} release in mouse dorsal root ganglion neurons is controlled by cytoplasmic and luminal Ca^{2+}. *Neuroscience.* 73:1061–1067.

Sitsapesan, R., and A.J. Williams. 1990. Mechanisms of caffeine activation of single calcium-release channels of sheep cardiac sarcoplasmic reticulum. *J. Physiol.* 423:425–439.

Sun, X.H., F. Protasi, M. Takahashi, H. Takeshima, D.G. Ferguson, and C. Franzini-Armstrong. 1995. Molecular architecture of membranes involved in excitation-contraction coupling of cardiac muscle. *J. Cell Biol.* 129:659–671.

Sutko, J.L., and J.A. Airey. 1996. Ryanodine receptor Ca^{2+} release channels: does diversity in form equal diversity in function? *Physiol. Rev.* 76:1027–1071.

Swenson, R.P., Jr., and C.M. Armstrong. 1981. K^+ channels close more slowly in the presence of external K^+ and Rb^+. *Nature.* 291:427–429.

Taschenberger, H., and R. Grantyn. 1998. Interaction of calcium-permeable non-N-methyl-D-aspartate receptor channels with voltage-activated potassium and calcium currents in rat retinal ganglion cells in vitro. *Neuroscience.* 84:877–896.

Thevenod, F., and S.W. Jones. 1992. Cadmium block of calcium current in frog sympathetic neurons. *Biophys. J.* 63:162–168.

Usachev, Y.M., and S.A. Thayer. 1997. All-or-none Ca^{2+} release from

intracellular stores triggered by Ca^{2+} influx through voltage-gated Ca^{2+} channels in rat sensory neurons. *J. Neurosci.* 17:7404–7414.

Vergara, C., R. Latorre, N.V. Marrion, and J.P. Adelman. 1998. Calcium-activated potassium channels. *Curr. Opin. Neurobiol.* 8:321–329.

Verkhratsky, A., and A. Shmigol. 1996. Calcium-induced calcium release in neurones. *Cell Calcium.* 19:1–14.

Wakamori, M., M. Strobeck, T. Niidome, T. Teramoto, K. Imoto, and Y. Mori. 1998. Functional characterization of ion permeation pathway in the N-type Ca^{2+} channel. *J. Neurophysiol.* 79:622–634.

Wang, G.Y., D.W. Robinson, and L.M. Chalupa. 1998. Calcium-activated potassium conductances in retinal ganglion cells of the ferret. *J. Neurophysiol.* 79:151–158.

Wang, Q., R.C. Hogg, and W.A. Large. 1992. Properties of spontaneous inward currents recorded in smooth muscle cells isolated from the rabbit portal vein. *J. Physiol.* 451:525–537.

Werblin, F.S., and J.E. Dowling. 1969. Organization of the retina of the mudpuppy, Necturus maculosus. II. Intracellular recording. *J. Neurophysiol.* 32:339–355.

Winegar, B.D., R. Kelly, and J.B. Lansman. 1991. Block of current through single calcium channels by Fe, Co, and Ni. Location of the transition metal binding site in the pore. *J. Gen. Physiol.* 97: 351–367.

Wisgirda, M.E., and S.E. Dryer. 1994. Functional dependence of Ca^{2+}-activated K^+ current on L- and N-type Ca^{2+} channels: differences between chicken sympathetic and parasympathetic neurons suggest different regulatory mechanisms. *Proc. Natl. Acad. Sci. USA.* 91:2858–2862.

Woodhull, A.M. 1973. Ionic blockage of sodium channels in nerve. *J. Gen. Physiol.* 61:687–708.

Yoon, Y.H., K.H. Jeong, M.J. Shim, and J.Y. Koh. 1999. High vulnerability of GABA-immunoreactive neurons to kainate in rat retinal cultures: correlation with the kainate-stimulated cobalt uptake. *Brain Res.* 823:33–41.

Zhang, J.F., A.D. Randall, P.T. Ellinor, W.A. Horne, W.A. Sather, T. Tanabe, T.L. Schwarz, and R.W. Tsien. 1993. Distinctive pharmacology and kinetics of cloned neuronal Ca^{2+} channels and their possible counterparts in mammalian CNS neurons. *Neuropharmacology.* 32:1075–1088.

ZhuGe, R., R.A. Tuft, K.E. Fogarty, K. Bellve, F.S. Fay, and J.V. Walsh, Jr. 1999. The influence of sarcoplasmic reticulum Ca^{2+} concentration on Ca^{2+} sparks and spontaneous transient outward currents in single smooth muscle cells. *J. Gen. Physiol.* 113: 215–228.

Zorumski, C.F., L.L. Thio, G.D. Clark, and D.B. Clifford. 1989. Calcium influx through N-methyl-D-aspartate channels activates a potassium current in postnatal rat hippocampal neurons. *Neurosci. Lett.* 99:293–299.

Zucchi, R., and S. Ronca-Testoni. 1997. The sarcoplasmic reticulum Ca^{2+} channel/ryanodine receptor: modulation by endogenous effectors, drugs and disease states. *Pharmacol. Rev.* 49:1–51.